Tunica Vaginalis Thickening, Hemorrhagic Infiltration and Inflammatory Changes in 8 Children with Primary Hydrocele; Reactive Mesothelial Hyperplasia? A Prospective Clinical Study

Ioannis Patoulias[1], Evangelia Rachmani[1], Maria Kalogirou[2], Kyriakos Chatzopoulos[3], Dimitrios Patoulias[4],*

ABSTRACT

The aim of this study is to describe an entity of primary hydrocele accompanied with fibrosis, thickening and hemorrhagic infiltration of parietal layer of tunica vaginalis (PLTV).

During a 4-year period (2011–2014), 94 boys (2.5–14 years old) underwent primary hydrocele repair. Hydrocele was right sided in 55 (58.5 %), left sided in 26 (28.7%) and bilateral in 12 patients (13.8%). Eighty three out of 94 patients (88.30%) had communicating hydrocele and the rest eleven patients (11.7%) had non-communicating. Our case group consists of 8 patients (8.51%) based on operative findings consistent with PLTV induration, thickening and hemorrhagic infiltration. Preoperative ultrasonography did not reveal any pathology of the intrascrotal structures besides hydrocele. There weren't hyperechoic reflections or septa within the fluid. Evaluation of thickness of the PLTV was not feasible. Presence of lymph or exudate was excluded after fluid biochemical analysis. Tunica vaginalis histological examination confirmed thickening, hemorrhagic infiltration and inflammation, while there was absence of mesothelial cells. Immunochemistry for desmin was positive, excluding malignant mesothelioma.

One patient underwent high ligation of the patent processus vaginalis and PLTV sheath fenestration, but one year later, he faced a recurrence. An elective second surgery was conducted via scrotal incision and Jaboulay operation was performed. The latter methodology was our treatment choice in other 7 out of 8 patients. During a 2-year postoperative follow-up, no other patient had any recurrence. We conclude that in primary hydrocele with macroscopic features indicative of tunica vaginalis inflammation, reversion of the tunica should be a part of operative strategy instead of sheath fenestration, in order to minimize the recurrence.

KEYWORDS

hydrocele; boy; tunica vaginalis; inflammation; thickening; fibrosis; hemorrhagic infiltration; Lord Technique

AUTHOR AFFILIATIONS

[1] 1st Department of Pediatric Surgery, Aristotle University of Thessaloniki, General Hospital "G. Gennimatas", Thessaloniki, Greece
[2] 4th Department of Internal Medicine, Aristotle University of Thessaloniki, Hippokration General Hospital, Greece
[3] Department of Pathology, General Hospital "G. Gennimatas", Thessaloniki, Greece
[4] Department of Internal Medicine, General Hospital of Veria, Veria, Greece
* Corresponding author: M. Alexandrou 3B, Peuka, Thessaloniki, 57010, Greece; e-mail: dipatoulias@gmail.com

INTRODUCTION

Hydrocele in childhood is divided into primary and secondary, based upon pathophysiology. Primary hydrocele is further divided into neonatal or congenital, communicating and closed or adult type or non-communicating (1).

Secondary hydrocele can develop due to inflammatory disorders (epididymitis, epididymo-orchitis), torsion of the testicle or embryonic tissue, inguinal hernia repair or varicocelectomy, hypoproteinemia in a systemic disease, traumatic disorders or tumours of intrascrotal structures. In the developing countries, parasitosis (lymphatic filariasis, Wuchereria bancrofti, scrotal schistosomiasis, etc.) usually causes secondary hydrocele (2).

We treated 8 patients with primary hydrocele in which fibrosis, thickening and hemorrhagic infiltration of parietal tunica vaginalis of the testicle were present. Thus, through this prospective clinical study, we aim at presenting the characteristic features of this "unknown" entity affecting tunica vaginalis, in order to facilitate the early recognition and the appropriate therapeutic approach of those patients.

MATERIALS AND METHODS

Over a 4-year period (2011–2014), 94 boys underwent hydrocele repair, due to primary hydrocele. The patients' ages ranged from 2.5 years to 14 years (mean 3.6 years). Primary hydrocele was right sided in 55 patients (58.5 %), left sided in 26 patients (28.7%) and bilateral in 12 patients (13.8%). Two incidents of secondary hydrocele were excluded.

Diagnosis of hydrocele is clinical and can be confirmed by ultrasonography. It is essential to clarify the onset of the scrotal swelling, while taking medical history from the parents, in order to confirm any fluctuation in size, which is an indication of primary (communicating) hydrocele.

During physical examination, we assessed the position, the turgidity and the size of the testicles, the silk-glove (or string) sign, the presence of tenderness or pain during palpation and the presence of palpable nodules on the scrotal wall or intrascrotal structures. Transillumination is also an additional method of clinical examination that should be performed if sonography is not available.

Performance of scrotal ultrasonography (US) facilitates the detection of position, size and structure of testicles and epididymis, the determination of echotexture of fluid and the evaluation of the presence of septa within the tunica vaginalis cavity and the diameter of processus vaginalis at the level of the internal inguinal ring.

After the performance of the typical preoperative tests, all the patients underwent elective surgery under general endotracheal anesthesia. Eighty three patients (88.3%) had communicating hydrocele, while 11 (11.70%) had non-communicating. After dissection of the anterior surface of tunica vaginalis, induration, thickening and hemorrhagic infiltration of it were the main macroscopic features in 8 patients. These intraoperative findings were in fact the determinants of our study subgroup.

RESULTS

Clinical and imaging findings of the 8 patients are presented in the tables 1 and 2 respectively. Classification of the patients was made based upon their age, in an ascending order (tables 1–3).

Ultrasonographic examination did not reveal any pre-existing or concomitant pathology of the intrascrotal structures, while there were no hyperechoic reflections or septa within the hydrocele fluid. Evaluation of the thickness of the parietal layer of tunica vaginalis was not feasible.
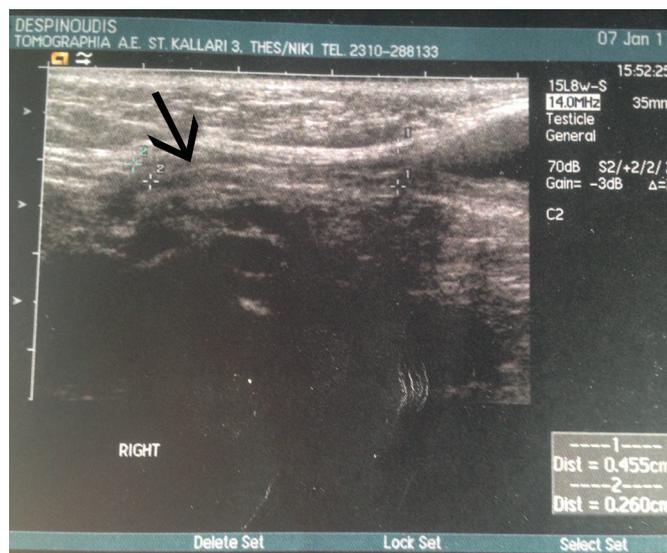

Fig. 1 Diameter of PV (2.6 mm) at the level of the internal inguinal ring in the 4th patient of our study group (black arrow).

Tab. 1 Clinical findings in the study group.

S/n	Onset of the scrotal swelling	Fluctuation in size detected from parents	Silk sign glove	Transillumination	Co-morbidity
1	From birth	Fluctuating	Yes	Ambiguous	No
2	From birth	Fluctuating	Yes	Ambiguous	No
3	From birth	Fluctuating	Yes	Ambiguous	No
4	From birth	Stable	Yes	No	No
5	From birth	Stable	Yes	No	No
6	From 7 years	Increasing	No	No	No
7	From 11 years	Increasing	No	No	No
8	From 9 years	Increasing	No	No	No

Tab. 2 Range of processus vaginalis (PV) at the level of the internal inguinal ring in the study group at ultrasonographic evaluation.

S/n	Diameter of processus vaginalis at the level of the internal inguinal ring (mm)
1	3.1
2	4
3	3.6
4	2.6
5	4
6	Closed
7	Closed
8	Closed

The first patient detected (5th patient in tables 1, 2, 3) underwent high ligation of the processus vaginalis with-'window' creation (sheath fenestration technique). Once the hydrocele was repaired, recurrence occurred within the following months and a second surgery was performed via scrotal incision and PLTV was reversed (Jaboulay technique) (Figure 2).

The rest 7 patients were treated with reversion and without excision of tunica vaginalis (Jaboulay technique, table 3, figures 3–4).

We also took tissue biopsy from the tunica vaginalis for histopathological evaluation and we collected fluid for biochemical and cytopathological examination. Presence of lymph or exudate was excluded by biochemical analysis.

Fig. 3 Notice the punctuated and scattered longitudinal hemorrhagic infiltration as well as thickening of the parietal layer of tunica vaginalis (4th patient).

Fig. 2 After opening of the anterior surface of tunica vaginalis, via scrotal incision (5th patient of tables 1, 2, 3), thickening and hemorrhagic infiltration of the parietal layer of tunica vaginalis were found (second operation).
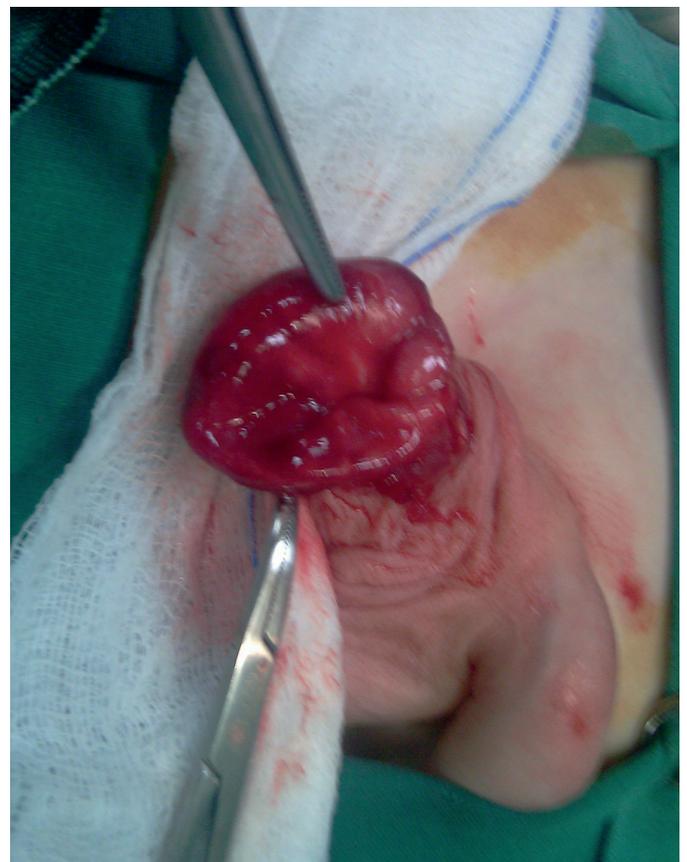

Fig. 4 Sixth patient of our study group. PLTV hemorrhagic infiltration.

Tab. 3 Analysis of 8 cases of primary hydrocele with hemorrhagic infiltration of parietal tunica vaginalis.

S/n	Age (years)	Position	Approach	PPV	Surgical procedure	Recurrence	Treatment
1	2.5	Right	Inguinal	Yes	high ligation of the processus vaginalis and reversion of the tunica vaginalis	No	
2	4	Right	Inguinal	Yes	high ligation of the processus vaginalis and reversion of the tunica vaginalis	No	
3	5	Left	Inguinal	Yes	high ligation of the processus vaginalis and reversion of the tunica vaginalis	No	
4	6	Right	Inguinal	Yes	high ligation of the processus vaginalis and reversion of the tunica vaginalis	No	
5	7	Right	Inguinal	Yes	high ligation of the processus vaginalis and sheath fenestration technique	Yes	reversion of the PLTV via scrotal incision (Jaboulay technique)
6	10	Left	Scrotal	No	reversion of the tunica vaginalis	No	
7	12	Right	Scrotal	No	reversion of the tunica vaginalis	No	
8	12	Left	Scrotal	No	reversion of the tunica vaginalis	No	
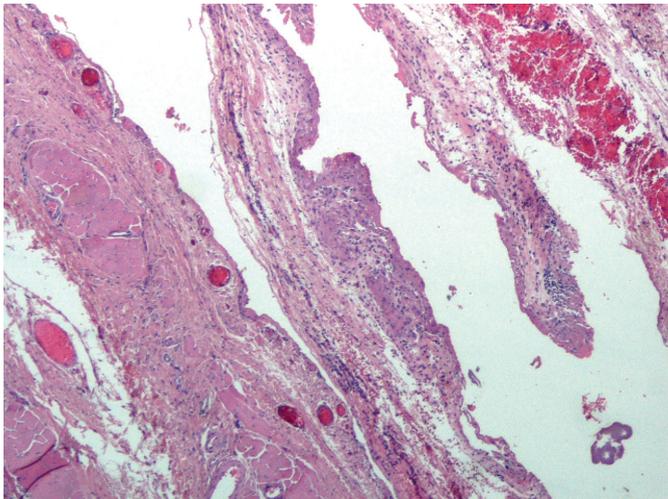
Fig. 5 Fifth patient of our study group: thickening, fibrosis and chronic inflammation of tunica vaginalis.
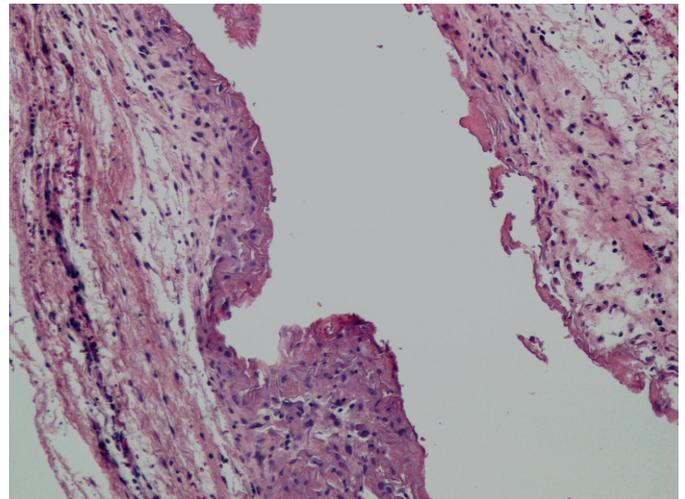
Fig. 6 Fifth patient of our study group: absence of mesothelial cells from the inner side of the tunica vaginalis, while dense fibrosis and infiltration by inflammatory cells are present.

Cytopathological examination excluded the presence of tumor cells or leukocytes. Histopathological examination of the tissue biopsies of the tunica vaginalis confirmed the presence of thickening – accompanied by intense fibroblastic activity –, absence of mesothelial cells from the inner side of the tunica vaginalis, hemorrhagic infiltration and inflammatory cells (figures 5, 6). Then immunohistochemical examination for desmin was found to be positive.

During a 2-year post-operative follow-up, on a 3-month basis, none of our patients had any recurrence. Ultrasonography was performed in all patients one year after the surgery. No abnormalities in the testicular parenchyma or size were found.

DISCUSSION

Pediatric surgeon should emphasize on the subject etiology when treating a boy with secondary hydrocele (3). In this prospective clinical study, cases of secondary hydrocele were excluded. During preoperative approach of a pediatric patient with hydrocele, the surgeon might come across various unusual findings, which may require a more thorough evaluation of the appropriate surgical procedure.

Prior to elective surgery, not only does clinical examination play an important role (thorough medical history and physical examination), but imaging modalities as well (scrotal and inguinal ultrasonography), which can add essential information regarding secondary hydrocele. When talking about secondary hydrocele, the clinician should mainly focus on: parasitic infections (filariasis, shistosomiasis), tuberculosis, syphilis, brucellosis, parotitis, autoimmune diseases (Ehlers Danlos Syndrome), nephrotic syndrome, chronic kidney disease, previous scrotal trauma, inflammatory intrascrotal structures, previous surgery, serositis due to systemic inflammatory response, testicular or paratesticular mass, and hydrocephalus in the presence of a ventriculoperitoneal shunt (4, 5).

None of our patients faced significant changes in size, which is indicative of malignancy, such as malignant mesothelioma of the tunica vaginalis or paratesticular rhabdomyosarcoma (5, 6).

Hydrocele repair should always be made on an elective basis and not urgently, in order the complete diagnostic approach to be made and the cases of secondary hydrocele to be excluded.

During physical examination, we assessed the position, the turgidity and the size of the testicles, the silk-glove (or string) sign, the presence of tenderness or pain during palpation and the presence of palpable nodules on the scrotal wall or intrascrotal structures. Transillumination was also conducted as an additional diagnostic method. As inguinoscrotal hernia along with the presence of intestinal loop cannot be excluded, positive transillumination should always be interpreted along with the rest objective clinical findings (3). In contrast, as found in 5 patients of our study group, negative transillumination could be evaluated as related with the thickening of the visceral tunica vaginalis intraoperatively (7).

Ultrasonographic depiction of the thickening of the tunica vaginalis was not feasible in any of our patients. Contrast Enhanced Sonography (CEUS) after bolus intravenous injection of contrast media, which is the most appropriate imaging modality, was not available in our Department (8). Depiction of tunica vaginalis thickening via high-resolution ultrasonography could contribute to preoperative diagnosis. Further appropriate clinical studies are required, in order to investigate and establish its use in clinical practice.

No nodules -solid or mottled and calcified- were seen within the thickened visceral tunica vaginalis, a finding indicative of a reactive fibro-inflammatory reaction. Ultrasonography did not reveal the presence of a single nodule or multinodular thickening of the tunica vaginalis (9). Nonetheless, the pathogenesis of this reaction still remains obscure. It is usually associated with history of prior trauma, Schistosoma Haematobium infection and HIV infection (10, 11, 12). In case of Schistosoma Haematobium infection, apart from the thickening of visceral tunica vaginalis, ultrasonography would also depict the presence of septa within the tunica vaginalis cavity (multicystic hydrocele) and scattered echoes, as well (9).Ultrasonography did not reveal any focal linear calcification in the inner surface of the tunica vaginalis that would be indicative of diffuse fibrous pseudotumor or fibromatous periorchitis (13).

The "classic" therapy of communicating hydrocele is the closure of the communication between the peritoneal cavity and the cavity defined by the parietal and the visceral layer of tunica vaginalis, by inguinal approach (9). The treatment of choice is the ligation of PPV at the level of the internal inguinal ring, along with incision of the outer layer of the hydrocele sac and creation of a "window" in the parietal tunica vaginalis (sheath fenestration) (14, 15).

Cases of abdominoscrotal hydrocele, could be corrected via scrotal approach (16, 17, 18).

From our study group, recurrence seen in our first patient, who had undergone high ligation of the PPV and "window" creation in the parietal layer of tunica vaginalis, was an unexpected complication and may be associated with the abnormal function of mesothelial lining. The latter may result either from fluid overproduction or failure of the mesothelial lining to reabsorb the fluid or both. Ozdilek et al. and Rinker et al. consider a non-communicating hydrocele as idiopathic, without associating the subject pathophysiological process with intraoperative findings such as the inflammatory changes of the parietal layer of tunica vaginalis (19, 20).

Rinker et al. and Allen suggest that a defective mechanism of lymphatic drainage develops in pediatric patients with hydrocele, finally affecting the drainage of the collected transudate (20). In our study group, collected fluid did not contain lymph in any of our patients.

Ku et al. consider as inappropriate the creation of a "window" in the parietal layer of tunica vaginalis, as adhesions develop gradually leading finally to "window's" closure. In those cases, recurrence rate of hydrocele reaches up to 85% (21).

Under this consideration, a more radical surgical intervention such as a partial excision and partial reversion of the tunica vaginalis was implemented. In our study group, reversion without excision of the tunica vaginalis was carried out in 7 patients (Jaboulay operation).

Diagnosis of hydrocele was based upon physical examination and imaging studies in the preoperative period, while biochemical and cytologic examination of hydrocele's fluid and histopathological examination of tissue biopsy taken from the tunica vaginalis completed postoperatively the diagnostic approach. After thorough evaluation of the above, no concomitant pathology was identified in any of our patients.

After evaluating the intraoperative macroscopic features and the histopathologic characteristics and excluding the presence of any concomitance, we made the possible diagnosis of tunica vaginalis mesothelium hyperplasia or reactive mesothelial hyperplasia (22–24). Reactive mesothelial hyperplasia is the most prominent diagnosis. Presence of primary hydrocele, absence of invasive character, absence of participation of the rest scrotal layers in the pathology, absence of lymphocytic infiltration and positive for desmin immunohistochemical reaction constitute the above diagnosis (22, 24–27).

There was no indication for further immunohistochemical staining (EMA, p53, GLUT-1, IMP-3) in order to exclude the presence of malignant mesothelioma of the tunica vaginalis. Immunohistochemical staining positive for EMA, p53, GLUT-1, IMP-3 and negative for desmin is indicative of malignant mesothelioma arising from the tunica vaginalis of the testis (28, 29). In cases when differential diagnosis is still ambiguous, DNA ploidy can distinguish some borderline lesions (30).

The differential diagnosis between reactive mesothelial hyperplasia and mesothelioma should always be carefully made. Despite the extreme rarity of mesothelioma during childhood, de Lima et al. report a case of a 15-year-old boy with secondary hydrocele and malignant mesothelioma as the etiologic substrate (31).

However, according to the study of Tolhurst et al., no malignancy can be ruled out by the absence of cellular atypia. The authors present a case of concomitance of uni-

lateral atypical reactive mesothelial hyperplasia and well differentiated mesothelioma contralaterally (32). They therefore consider the presence of invasive behavior as significant parameter, strongly indicative of malignancy. Based upon the histologic examination of the tissue biopsies taken from the parietal layer of the tunica vaginalis, there was no indication of true invasion or prominent infiltration in our study group.

CONCLUSIONS

1. When inflammatory changes of tunica vaginalis are found as an intraoperative finding in the context of primary hydrocele surgical repair, it is critical to evaluate whether they are secondary or not. Malignant mesothelioma must always be excluded, based upon cytological examination of the fluid and immunohistochemical examination of the tissue biopsy for desmin at initial approach.

2. In communicating hydrocele cases with macroscopic features indicative of inflammation of PTLV, high ligation of the PPV and tunica vaginalis sheath fenestration are accompanied with recurrence. Thus the "classic" operative technique is considered as insufficient. On the contrary, high ligation of PPV along with Jaboulay technique minimizes the recurrence rate.

3. In cases of noncommunicating or adult type hydrocele, scrotal approach and reversion of PLTV lead to the minimization of the recurrence rate.

REFERENCES

1. Dave J. Cause and management of hydrocele: a review article. Indian J of Applied Research 2015; 5(10): 117–8.
2. DeVries C. The role of urologist in the treatment and elimination of lymphatic filariasis worldwide. BJU Int 2002; 89(1): 37–43.
3. Tahir MS. Hydrocele. Indep Rev 2014; 16(4–6): 145–50.
4. Tarantino L, Giorgio A, de Stefano G, Farella N. Echo color Doppler findings in post pubertal mumps epididymo orchitis. J Ultrasound Med 2001; 20: 1189–95.
5. Zaslau S, Perlmutter AE, Farivar-Mohseni H, Chang WW, Kandzari SJ. Rhabdomyosarcoma of tunica vaginalis masquerading as hydrocele. Urol 2005; 65: 1001.
6. Cimador M, Castagnetti M, De Grazia E. Management of hydrocele in adolescent patients. Nat Rev Urol 2010; 7(7): 379–85.
7. Rubenstein A, Dogra VS, Seftel AD, Resnick MI. Benign intrascrotal lesions. J Urol 2004; 171: 1765–72.
8. Puttermans T, Ingabire MI, Jorion JL, Draguet AP. Fibrous pseudotumor of the tunica vaginalis: contrast enhanced sonography with pathologic correlation. JBR-BTR 2014; 97: 259–61.
9. Garriga V, Serrano A, Marin A, et al. US of tunica vaginalis testis: Anatomic relationships and pathologic conditions. Radiographics 2009; 29: 2017–32.
10. Mostophi FK, Price EB. Tumors of the male genital system. In: Atlas of tumor pathology, 2nd series, Fascicle 8, Wasington DC: Armed Forces Institute Pathology, 1973: 151.
11. Parker PM, Pugliese JM, Allen RC. Benign fibrous pseudotumor of tunica vaginalis testis. Urol 2006; 68: 427e17–e19.
12. Navai N, Yap RL, Gupta R, Fraser TG, Gonzalez CM. Inflammatory pseudotumor of the testis: a novel presentation of acute retroviral syndrome. Int J Urol 2005; 12: 424–6.
13. White WM, Hilsenbeck J, Waters WB. Fibromatous periorchitis of testis. Urology 2006; 67(3): 623.e15–6.
14. Holcomb GW, Murhy JP, Ostlie DJ. Ashcraft's Pediatric Surgery. 6th edition. New York: Elsevier Saunders, 2014, Chapter 50, pp 679–88.
15. Andrews EW. The "Bottle Operation" method for the radical cure of hydrocele. Ann Surg 1907; 46: 915–8.
16. Belman AB. Abdominoscrotal hydrocele in infancy: a review and presentation of the scrotal approach for correction. J Urol 2001; 165(1): 225–7.
17. Koutsoumis G, Patoulias I, Kaselas C. Primary new-onset hydroceles presenting in late childhood and pre-adolescent patients resemble the adult type hydrocele pathology. J Pediatr Surg 2014; 49: 1656–8.
18. Wilson JM, Aaronson DS, Schrader R, Baskin LS. Hydrocele in the pediatric patient: inguinal or scrotal approach? J Urol 2008; 180: 1724–8.
19. Ozdilek S. The pathogenesis of idiopathic hydrocele and a simple operative technique. J Urol 1957; 77: 282–4.
20. Rinker J, Allen L. A lymphatic defect in hydrocele. Am Surg 1951; 17: 681–6.
21. Ku JH, Kim M, Lee NK, Park YH. The excisional, plication and internal drainage techniques: a comparison of the results for idiopathic hydrocele. BJU Int 2001; 87: 82–4.
22. Algaba F, Mikuz G, Boccon-Gibod L, et al. Psudoneoplastic lesions of the testis and paratesticular structures. Virchows Archiv 200; 451(6): 987–97.
23. Perez-Ordonez B, Srigley JR. Mesothelial lesions of the paratesticular region. Semin Diagn Pathol 2000; 17: 294–306.
24. Colecchia M, Mikuz G, Algaba F. Rare tumors of the testis and mesothelial proliferation in the tunica vaginalis. Tumori 2012; 98: 270–3.
25. Erdogan S, Acikalin A, Zeren H, et al. Well-Differentiated Papillary Mesothelioma of the Tunica Vaginalis: A Case Study and Review of the Literature. Korean J Pathol 2014; 48(3): 225–8.
26. Bolen JW, Hammar SP, McNutt MA. Reactive and neoplastic serosal tissue. A light-microscopic, ultrastructural, and immunocytochemical study. Am J Surg Pathol 1986; 10: 34–47.
27. Tyagi G, Munn CS, Kiser LC, Wetzner SM, Tarabulcy E. Malignant mesothelioma of tunica vaginalis testis. Urol 1989; 34: 102–4.
28. Chen JL, Hsu YH. Malignant mesothelioma of the tunica vaginalis testis: a case report and literature review. Kaohsiung J Med Sci 2009; 25: 77–81.
29. Goel A, Agrawal A, Gupta R, Hari S, Dey AB. Malignant mesothelioma of the tunica vaginalis of the testis without exposure to asbestos. Cases J 2008; 1: 310.
30. Friedman MT, Gentile P, Tarectecan A, Fuchs A. Malignant mesothelioma: immunohistochemistry and DNA ploidy analysis as methods to differentiate mesothelioma from benign reactive mesothelial cell proliferation and adenocarcinoma in pleural and peritoneal effusions. Arch Pathol Lab Med 1996; 120(10): 959–66.
31. De Lima GR, De Oliveira VP, Reis PH, et al. A rare case of malignant hydrocele in a young patient. J Pediatr Urol 2009; 5(3): 243–5.
32. Tolhurst SR, Lotan T, Rapp DE, et al. Well-differentiated papillary mesothelioma occurring in the tunica vaginalis of the testis with contralateral atypical mesothelial hyperplasia. Urol Oncol 2006; 24: 36–9.

Electrodermal Activity Monitoring During Painful Stimulation in Sedated Adult Intensive Care Unit Patients: a Pilot Study

Theodoros Aslanidis[1],*, Vasilios Grosomanidis[2], †Konstantinos Karakoulas[3], Athanasios Chatzisotiriou[4]

ABSTRACT

Introduction-Aim: Newer methods, such as infrared digital pupillometry and electrodermal activity (EDA) measurement have been suggested as good alternatives for analgesia monitoring in critically ill patients. This study analyzed EDA changes due to pain stimulus in sedated adult critical care patients

Methods: Skin conductance variability, selected hemodynamic and respiratory parameters, Bispectral index (BIS) and ambient noise level, were monitored during 4 hour routine daytime in an adult ICU. 4h-Measurements were divided into 2 groups, based upon the sedation level of the patients: Group A – Ramsay Sedation Score 2–4 and Group B – Ramsay Sedation Score of 5–6. Selected recordings before and after pain stimulus were performed. The stimulus chosen was the pressure applied to nail bed for 10 sec, which was performed routinely during neurological examination. Patients' demographics, laboratory exams and severity scores were recorded. Pain status evaluation before every event was also performed by 2 independent observers via Critical Care Pain Observation Tool (CPOT) and Adult Non Verbal Pain Score (ANVPS)

Results: In both groups the rate of EDA changes was greater than other monitoring parameters: more in Group A than in Group B. Yet, the difference between groups was not statistically significant.

Conclusion: EDA measurements are greater to pain stimuli, than cardiovascular, respiratory or even BIS monitoring. These encouraging results suggest that, further studies are needed to better define EDA role in ICU.

AUTHOR AFFILIATIONS

[1] Intensive Care Unit, Department of Anesthesiology and Intensive Care Medicine, AHEPA General University Hospital, Thessaloniki, Greece
[2] Anesthesiologist, Cardiothoracic Anesthesia Unit, Department of Anesthesiology and Intensive Care Medicine, AHEPA General University Hospital, Thessaloniki, Greece
[3] Anesthesiologist, Department of Anesthesiology and Intensive Care Medicine, AHEPA General University Hospital, Thessaloniki, Greece
[4] Neurosurgeon, Laboratory of Physiology, Medical School, Aristotle University of Thessaloniki, Thessaloniki, Greece
* Correspondence author: 4 Doridos Street, Thessaloniki, 54633, Greece; e-mail: thaslan@hotmail.com

INTRODUCTION

Intensive Care Unit (ICU) environment is full of stimuli and patients may feel pain even at rest (1–2). Thus, pain should be routinely assessed in all adult ICU patients (3). Yet, pain evaluation is difficult, considering biases such as sedation, existence of delirium and lack of an objective monitor tool. Because vital signs' changes are not considered a reliable way for pain assessment (4) this symptom is usually assessed by using one of the existing behavioral scales. Current guidelines (3) support the use of the Behavioral Pain Scale (BPS) and the Critical-Care Pain Observation Tool (CPOT) for monitoring pain in different medical settings, including postoperative, trauma adult patients who are unable to self-report, and in those with intact motor function and observable behaviors.

Newer methods, such as infrared digital pupillometry and electrodermal activity (EDA) measurement have been suggested as good alternatives for analgesia monitoring (5–6). Both are based on the autonomic nervous system response to stimuli. The first records pupil's response dynamics while EDA is originated from the activation of sweat glands in the skin in response to stress or other stimuli.

Unfortunately, till the conduct of the present study, there were only few reports about EDA measurements in adult (7–9) or peadiatric (10–11) ICU environment. In adult patients, results were not conclusive. In pediatric population, the number of skin conductance fluctuations seems to be an objective supplement to the modified COMFORT sedation score for monitoring increased stress in artificially ventilated and circulatory stable children (10). Measurement of skin conductivity as an objective tool to measure pain and discomfort during invasive procedures despite the use of sedation and analgesia has also been reported in neonatal intensive care units' patients (11). Yet, the overall data are limited.

The present study analyzed EDA changes at palms during pain stimulus (pressure applied to nail bed) in adult sedated ICU patients. Simultaneously recordings of several other parameters were also used in the analysis.

METHODS

This prospective observational study was conducted at the adult general ICU, at AHEPA General University Hospital, Thessaloniki, Greece. The study is part of a thesis project, approved by AHEPA General University Hospital Research Committee and by No. 16/09-07-2013 General Assembly of Special Composition of Medical School, Aristotle University of Thessaloniki (Ref. No. 8220/10-07-2013).

Twenty five (25) measurements in critically ill patients under sedation, above 18 years old, were included in the study. Other inclusion criteria included administered mechanical ventilation > 24 h and constant sedation level under midazolam or propofol continuous intravenous infusion.

On the contrary, patients with Ramsay sedation score (RSS) 1, diagnosed or with history of hearing problems, psychiatric disorders, neurological diseases, neuropahty or myopathy, delirium, CNS or spinal cord injury, were excluded. Also as exclusion criteria were considered pregnancy, hemodynamic/respiratory instability, edema of the upper limbs (place of measurement) and the presence of sensitive electrical life-sustainable devices such as cardiac pace, renal replacement therapy devices, intra-abdominal aortal counterpulsation pump, extracorporeal membrane oxygenation and artificial liver.

Skin conductance (SC) variability, selected hemodynamic and respiratory parameters (HR – heart rate, VPC – ventricular premature contractions (number), STII – electrocardiographic ST wave deviation in II lead, SAP – systolic arterial pressure, MAP – mean arterial pressure, DAP – diastolic arterial pressure, RR – respiratory rate) were monitored during 4 hour routine daytime intensive care nursing and treatment (afternoon shift, measurements during 4:00 p.m. – 8:00 p.m.). Measurements were divided into 2 categories according to patient's sedation level: Group A – RSS 2–4 (na = 10) and Group B – RAS 5–6 (nb = 15). Dosing to achieve the given sedation level, although recorded, was not taken into account (since a point of interest was sedation level).

Med Storm Pain Monitor System (MED Storm® Innovation AS, Oslo, Norway) was used as SC monitor (12). Three single use Ag/Cl electrodes were attached at the palmar surface of the hand: on the thenar eminence (current), on the hypothenar eminence (measurement) and just below 2nd and 3rd digits (reference). In order to minimize artifacts, the hand least likely to move, with no intravenous or intra-arterial lines was chosen. SC was measured by alternating current of 66 Hz and an applied voltage of 50 mV. SC parameters recorded were: absolute SC (in μS), peaks/sec or number of SC fluctuations per second (NSCF), the average peak (AvP) (microSiemens seconds, μSs), the rate of increase or decrease from the start to the end of the measurement window (rise time, AvRT, in micro Siemens per second, μS/s), area huge peaks (ArHP) (μSs), area small peaks (ArSP) (μSs) and the larger of the two measures (referred as Area under curve- AUC, in μSs). Cut off for NSCF counting was >0.02 μS, the same used in relative pain monitoring literature (6). Signal quality <80% was considered artifact and the measurement was also excluded.

The stimulus chosen was pressure applied to nail bed for 10 sec; which was performed routinely during neurological examination (mentioned as "event").

Two measurement windows of interest were used: 1) 15 s before and 15 s (pre-set window by the given monitor for measuring effect of short lasting stimuli) after and 2) 60 s before and 60 s after (in order to average out the effect) Two independent observers evaluated pain 15 s before and 15 s after stimulus with Critical Care Observation Pain Tool (CPOT) and Adult Non Verbal Pain Scale (ANPS) (13).

Only those "events" that were within the aforementioned frames, were included for further analysis: 35 for both groups for the 15s window and 32 for the 60s window).

The rest of the parameters (HR, SAP, DAP, VPC, RR, STII) were monitored via Bedside Monitor BSM 9101K and Monitor CNS 9601 (Nihon Kohden® Ltd., Japan). Since

the above were suggested in the literature (17) as possible measures of stress, recordings were used as measure of comparison with SC parameters.

Though a bispectral index monitor device was available, clinical priority was given over research priority. Thus, Bispectral index monitor (BIS) (Covidien®, USA) was used in selected measurements (Group A: 12, Group B: 7).

Ambient noise level was measured at distance 30 cm from the head of the patient via Sound Level Meter GM13656 (Shenzhen Jumaoyuan Science & Technology® Co., China).

Data analysis was performed with MS Office Excel 2007 (Microsoft® Co, USA) and Rstudio IDE® v.1.00.136 (Rstudio Inc, USA) for R v.3.4.1 (R Foundation®, USA).

Two comparison designs were applied. The former examined acute changes before/after the noise stimulus, for each window, and the latter evaluated the range of change between the 2 groups. Shapiro-Francia normality test was performed for the parameters of interest and then paired Student t-test or Wilcoxon signed rank test was calculated. Results were presented as p value (Confidence Interval, CI). Statistical significance for p is set to $p < 0.05$ and CI level at 95%. CPOT score is presented as (s), while agreement between the 2 observers are evaluated with inter-rater reliability (*IRR*) and Lin concordance correlation coefficient ρc (with two-sided 95% Confidence Limits-CL).

RESULTS

General characteristic of patients in each group of measurements is illustrated in Table 1. Different averages of APACHE II score, Extended Glasgow Outcome Score (GOSE) and PaO2/FiO2 are partially explain the different sedation level. All measurements were conducted on white Caucasian patients. Ambient noise levels, 4 min before the start and during the "events" were: 57.5 (4.75) dB in Group

Tab. 1 General characteristics of the patients included finally in each group. Presented form: mean (SD), rounded to the nearest decimal. SOFA: Sequential Organ Failure Assessment (SOFA) Score.

	Group A	Group B		Group A	Group B
N measurem	10	15	APACHE II	15.4(1.55)	19.6(1.66)
Sex	♂ = 10, ♀ = 0	♂ = 9, ♀ = 6	SOFA	6.3(0.9)	7.9(0.4)
Age (years)	66.5(14.8)	63.8(10.9)	GOSE	6.4(0.9)	5.2(0.8)
Weight (kg)	90.6(15,1)	89.95(12.6)	t (°C)	37.1(0.3)	37(0.4)
BMI (kg/m^2)	28(1.65)	30.3(0.85)	PaO$_2$/FiO$_2$	294(69.3)	230(81.8)

Tab. 2 Main descriptive statistics and before/after comparison of the measurements during suction in 1st group sedation level: EDA parameters (ArHP – Area Huge Peaks, ArSP – Area Small Peaks, NFSC – Number of Fluctuation of SC, AvRT – Average Rise Time, AvP – Average Peaks, AUC – Area Under Curve, SC – Skin Conductance). B – Before stimulus, A – After stimulus. NA – non-significant change.

Group	A (RSS 3–4), n = 14 (15 s), 11 (60 s)				
Parameter→	ArHP (µSs)		ArSP (µSs)		NFSC (µSs)
window→	15 s	60 s	15 s	60 s	15 sec
B $\bar{\chi}$(s)	0	0	0.007(0.002)	0.001(0.003)	0.014(0.038)
A $\bar{\chi}$(s)	0.981(2.34)	6(17.61)	0.185(0.462)	0.31(0.02)	0.136(0.078)
P	0.009	0.0142	0.008	0.009	0.001
CI [95%]	[−4,−0.05]	[−30,−0.6]	[−0.9,−0.03]	[−1.24,−0.03]	[−0.16,−0.07]
Parameter→	NFSC (µSs)	AvRT		AvP	
window→	60 s	15 s	60 s	15 s	60 s
B $\bar{\chi}$(s)	0.009(0.022)	−0.002(0.008)	−0.001(0.003)	0.001(0.003)	0.002(0.004)
A $\bar{\chi}$(s)	0.071(0.059)	0.057(0.016)	0.018(0.006)	0.046(0.066)	0.038(0.042)
P	0.005	0.371	NA	0.0014	0.003
CI [95%]	[−0.1,−0.02]	NA	NA	[−0.1,−0.01]	[−0.07,−0.01]
Parameter→	AUC (µSs)		SC (µS)		
window→	15 s	60 s	15 s	60 s	
B $\bar{\chi}$(s)	0.007(0.002)	0.009(0.003)	5.051(5.09)	4.535(3.98)	
A $\bar{\chi}$(s)	0.997(2.33)	6(17.59)	5.098(5.095)	4.72(4.28)	
P	0.0038	0.005	0.0107	0.053	
CI [95%]	[−4.04,−0.05]	[−29.5,−0.7]	[−0.05,−0.002]	[−0.58,−0.0004]	
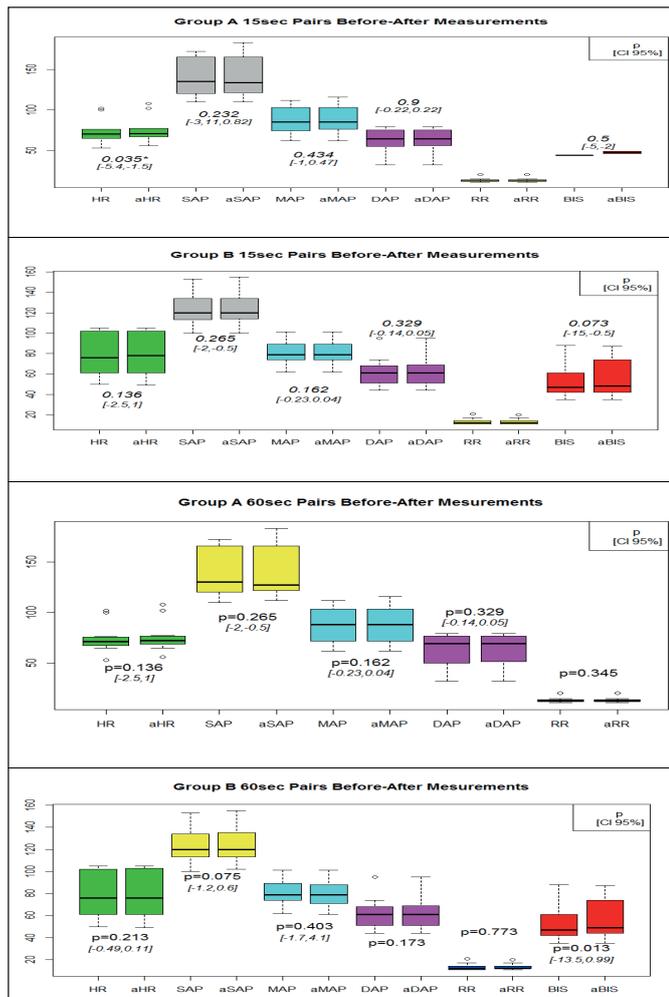
Graph 1 Box plots for the 15 s measurements for both groups. Comparison of before and after event (prefix a~ is used) values of several parameters are displayed, along with p value and 95% confidence interval. HR – heart rates, SAP – systolic arterial pressure, MAP – mean arterial pressure, DAP – diastolic arterial pressure, RR – respiratory rate, BIS – Bi-spectral index value. The 95% confidence interval is providing the range of the difference of the means falls in, with (1 – a = 0.05)% confidence. In cases that zero in included then we can't rule out the possibility that the means are equal, up to a 1 in 20 chance of having missed a difference.

A and 56.5 (2.62) dB in Group B. Hemoglobin and serum electrolytes were within normal limits for both groups.

During 15sec recording time, 14 pain "events" occurred in Group A (12 had also BIS monitor) and 21 in Group B (7 had also BIS monitor) that met inclusion criteria for further analysis. EDA parameters are displayed in Table 2 (Group A) and Table 3 (Group B), while the rest of the parameters are illustrated in Graph 1.

The mean percentage of change before/after the "event" is also displayed in table 4, where it is demonstrated the vast amount of EDA parameters change.

Agreement of the 2 observers in the evaluation of pain with CPOT and ANVPS scales before and during the stimulus, are presented in table 5. Both investigators assessed stimulus as light to moderately painful.

DISCUSSION

Results illustrated that EDA changes are much greater than the other parameters used. Only HR in Group A (15 s measurements) changed significantly ($p < 0.05$) in comparison with baseline values. On the contrary, all EDA parameters (with exception of SC) displayed a vast change due to the stimulus in both Groups, for both measurement windows. Lighter level of sedation in Group A may explain the greater range of change. Assessment of the stimulus via non-objective measures showed also good agreement of between the 2 observers.

In the present study, both Groups were similar both in age, weight and BMI. The same is true for main laboratory parameters. Ambient noise-an also recognized stress stimulus in ICU (14) – before the start and during the stimulus was similar in both groups. Sex may play a confounding role in EDA measurement because of monthly hormonal variations in women (15). However, the measurements in the present study were conducted in older women. In addition, laboratory studies in ambulatory setting have been inconclusive (16, 17).

Sleep quality has been connected in the literature with several diseases (18). Thus, quality of sleep between the two groups is possible contributing factor; however its effect on EDA measurements was not evaluated in the current study. EDA could be a serve as a tool to assess not only sleep and anesthesia in ICU, but also phenomena like consciousness fluctuation or dreaming during anesthesia in critically ill (19–20).

The relatively small number of measurements and the open, observational character of the study can also be considered as limitations. Further studies with bigger samples both in ICU patients with predefined criteria, will certainly reveal more information. These criteria could be patient based (e.g. pregnant women in ICU) or condition based (e.g. trauma brain injuries, post cardiac arrest, sepsis) or even neuro-psychological ICU related disorders (e.g. ICU delirium, postoperative cognitive dysfucntions) (21). Along with that, more strictly predefined stimuli are needed in order to have a clear idea of the role of EDA monitoring in adult ICU environment. Till now (2017), there is only one report about measurement of EDA changes in healthy volunteers due to a similar predefined stimulus (applying pressure to scapula) (22). The use of adequate analgesia and the type of sedative agent (e.g. propofol or dexmedetomidine) is a prospective that needs to be assessed too. The reports from pediatric patients may suggest EDA monitor as an analgesia monitor; but even them are few (23–26). The aforementioned reveal a huge range of challenges that remain to be met for ICU patients. A recent report evaluated EDA changes during endotracheal suction in sedated adult critical care patients and another one EDA monitoring during arterial blood pooling for arterial blood gases analysis in the same population: both with very interesting results (27–29).

Finally, one has to note that the exact role and physiological "reflection" of every of the aforementioned EDA parameters to the ANS activity is yet to be determined (6, 30) and that there are several ways of analyzing the EDA data, which also need to be kept in mind (30).

Tab. 3 Main descriptive statistics and before/after comparison of the measurements during suction in 2nd group sedation level: EDA parameters (ArHP – Area Huge Peaks, ArSP – Area Small Peaks, NFSC – Number of Fluctuation of SC, AvRT – Average Rise Time, AvP – Average Peaks, AUC – Area Under Curve, SC – Skin Conductance).

Group		B = (RSS 5–6), n = 21 (15 s, 60 s)				
Parameter→		ArHP (µSs)		ArSP (µSs)		NFSC (µSs)
window→		15 s	60 s	15 s	60 s	15 s
B	$\bar{\chi}$(s)	0.03(0.129)	0.039(0.146)	0	0.049(0.153)	0.01(0.025)
A	$\bar{\chi}$(s)	1.16(2.265)	4.47(7.44)	0.23(0.824)	0.622(1.456)	0.15(0.141)
P		0.0004	0.0002	0.0038	0.018	0.0001
CI [95%]		[−1.7,−0.37]	[−6.39,−1.2]	[−2,−0.03]	[−2.8,−0.02]	[−0.2,−0.09]
Parameter→		NFSC (µSs)	AvRT		AvP	
window→		60 s	15 s	60 s	15 s	60 s
B	$\bar{\chi}$(s)	0.01(0.029)	−0.002(0.01)	0	0.01(0.039)	0.002(0.006)
A	$\bar{\chi}$(s)	0.638(0.07)	0.01(0.0185)	0.001(0.006)	0.06(0.1)	0.561(0.085)
P		0.0001	0.0052	0.3741	0.0069	0.0004
CI [95%]		[−0.09,−0.02]	[−0.04,−0.01]	[−0.015,0.01]	[−0.11,−0.01]	[−0.08,−0.02]
Parameter→		AUC (µSs)		SC (µS)		
window→		15 s	60 s	15 s	60 s	
B	$\bar{\chi}$(s)	0.03(0.129)	0.054(0.171)	5.23(2.89)	5.251(2.91)	
A	$\bar{\chi}$(s)	1.15(2.273)	4.58(7.44)	5.27(2.923)	5.143(2.997)	
P		0.0003	0.0001	0.0463	0.513	
CI [95%]		[−1.6,−0.25]	[−6.3,−1.04]	[−0.08.−0.0006]	[−0.06,0.01]	

Tab. 4 Mean change (%) for every measured parameter. (ArHP – Area Huge Peaks, ArSP – Area Small Peaks, NFSC – Number of Fluctuation of SC, AvRT – Average Rise Time, AvP – Average Peaks, AUC – Area Under Curve, SC – Skin Conductance).

window	15 s	60 s	15 s	60 s	15 s	60 s	15 s	60 s
% Δ	ArHP		ArSP		NFSC		SC	
Group A	17600	NA	107.7	24300	NA	566.67	0.54	2.03
Group B	3868	7189	NA	21.6	281	92.43	0.75	−2.3
% Δ	AvRT		AvP		AUC			
Group A	−433	−300	1050	750	80600	~5000		
Group B	−100	NA	187	250	3868	~5000		

Tab. 5 Agreement of the 2 observes of the CPOT and ANVPS recordings.

Before	Group A (15 s)			Group B (15 s)		
Score	IRR* (%)	ρ_c**	ρ_c CL 95%	IRR* (%)	ρ_c**	ρ_c CL 95%
CPOT	71.42	0.6923	[0.29,088]	100	1	NA
ANVPS	78.57	0.8421	[0.59,0.94]	100	1	NA
During						
CPOT	92.85	0.9625	[0.90,0.98]	61.9	0.71	[0.47,0.85]
ANVPS	85.91	0.92	[0.81,0.96]	66.67	0.7487	[0.52,0.87]

* Inter rater reliability
** Lin concordance correlation coefficient (with two-sided 95% Confidence Limits)

CONCLUSION

EDA measurements are more sensitive to pain stimulus in sedated adult ICU patients, than cardiovascular, respiratory or even BIS monitoring; thus serving as a more sensitive index of stimulus-induced pain. However, future studies are needed in order to define EDA role as pain or stress monitor and to clarify possible specific stimulus EDA response patterns in all group of ICU patients.

CONFLICTS OF INTEREST

The authors declare that there is no conflict of interest.

REFERENCES

1. Chanques G, Sebbane M, Barbotte E, Viel E, Eledjam JJ, Jaber S. A prospective study of pain at rest: Incidence and characteristics of an unrecognized symptom in surgical and trauma versus medical intensive care unit patients. Anesthesiology 2007; 107: 858–60.
2. Gélinas C. Management of pain in cardiac surgery ICU patients: Have we improved over time? Intensive Crit Care Nurs 2007; 23: 298–303.
3. Medicine. Clinical Practice Guidelines for the Management of Pain, Agitation, and Delirium in Adult Patients in the Intensive Care Unit. Crit Care Med 2013; 41: 263–306.
4. Gélinas C, Johnston C. Pain assessment in the critically ill ventilated adult: Validation of the Critical-Care Pain Observation Tool and physiologic indicators. Clin J Pain 2007; 23: 497–505.
5. Aslanidis T, Kontogounis G. Perioperative digital pupillometry – the future? Greek e J Perioper Med 2015; 13(b): 24–40.
6. Aslanidis T. Electrodermal activity: Applications in Perioperative Care. Int J Med Res Health Sci 2014; 3(3): 687–95.
7. Gunther AC, Bottai M, Schandl AR, Storm H, Rossi P, Sackey PV. Palmar skin conductance variability and the relation tostimulation, pain and the motor activity assessment scale inintensive care unit patients. Crit Care 2013; 17: R51.
8. Günther AC, Schandl AR, Berhardsson J, et al. Pain rather than induced emotions and ICU sound increases skin conductance variability in healthy volunteers. Acta Anaesthesiol Scand 2016; 60(8): 1111–20.
9. Gjerstad AC, Storm H, Hagen R, Huiku M, Qvigstad E, Raeder J. Skin conductance or entropy for detection of non-noxious stimulation during different clinical levels of sedation. Acta Anaesthesiol Scand 2007; 51: 1–7.
10. Karpe J, Misiołek A, Daszkiewicz A, Misiołek H. Objective assessment of pain-related stress in mechanically ventilated newborns based on skin conductance fluctuations. Anaesthesiol Intensive Ther 2013; 45(3): 134–7.
11. Gjerstad AC, Wagner K, Henrichsen T, Storm H. Skin conductance versus the modified COMFORT sedation score as a measure of discomfort in artificially ventilated children. Pediatrics 2008; 122(4): e848–53.
12. Med Storm Monitor User Manual v1.0 English MA001-25, Part Number 4001, Med Storm Innovation AS, Oslo, 2010.
13. Gelinas C, Tousignant-Laflamme Y, Tanguay A, Bourgault P. Exploring the validity of the bispectral index, the Critical-Care Pain Observation Tool and vital signs for the detection of pain in sedated and mechanically ventilated critically ill adults: a pilot study. Intensive Crit Care Nurs 2011; 27(1): 46–52.
14. Putz-Maidl C, MacAndrew SN, Leske JS. Noise in ICU: Sound levels can be harmful. Nurs Crit Care 2014; 9(5): 29–35.
15. Goldstein JM, Jerram M, Poldrack R, et al. Hormonal cycle modulates arousal circuitry in women using functional magnetic resonance imaging. J Neurosci 2005; 25(40): 9309–16.
16. Doberenz S, Roth WT, Maslowski NI, Wollburg E, Kim S. Methodological Considerations in Ambulatory Skin Conductance Monitoring. Int J Psychophysiology 2011; 80(2): 87–95.
17. Carrillo E, Moya-Albiol L, González-Bono E, Salvador A, Ricarte J, Gómez-Amor J. Gender differences in cardiovascular and electrodermal responses to public speaking task: the role of anxiety and mood states. Int J Psychophysiol 2001; 42(3): 253–64.
18. Tobaldini E, Costantino G, Solbiati M, et al. Sleep, sleep deprivation, autonomic nervous system and cardiovascular diseases. Neurosci Biobehav Rev 2017; 74(Pt B): 321–29.
19. Cascella M, Schiavone V, Muzio MR, Cuomo A. Consciousness fluctuation during general anesthesia: a theoretical approach to anesthesia awareness and memory modulation. Curr Med Res Opin. 2016; 32(8):1351–9.
20. Cascella M, Fusco R, Caliendo D, et al. Anesthetic dreaming, anesthesia awareness and patient satisfaction after deep sedation with propofol target controlled infusion: A prospective cohort study of patients undergoing day case breast surgery. Oncotarget 2017; 8(45): 79248–56.
21. Cascella M, Muzio MR, Bimonte S, Cuomo A, Jakobsson JG. Postoperative delirium and postoperative cognitive dysfunction: updates in pathophysiology, potential translational approaches to clinical practice and further research perspectives. Minerva Anestesiol 2018; 84(2): 246–260.
22. Kim JH, Park GC, Baik SW, Reon GR. Electrodermal Activity at palms according to Pressure Stimuli applied to the Scapula. J Korea Multimed Soc 2016; 19(7): 1137–45.
23. Günther AC, Schandl AR, Berhardsson J, et al. Pain rather than induced emotions and ICU sound increases skin conductance variability in healthy volunteers. Acta Anaesthesiol Scand 2016; 60(8): 1111–20.
24. Gjerstad AC, Storm H, Hagen R, Huiku M, Qvigstad E, Raeder J. Skin conductance or entropy for detection of non-noxious stimulation during different clinical levels of sedation. Acta Anaesthesiol Scand 2007; 51: 1–7.
25. Karpe J, Misiołek A, Daszkiewicz A, Misiołek H. Objective assessment of pain-related stress in mechanically ventilated newborns based on skin conductance fluctuations. Anaesthesiol Intensive Ther 2013; 45(3): 134–7.
26. Gjerstad AC, Wagner K, Henrichsen T, Storm H. Skin conductance versus the modified COMFORT sedation score as a measure of discomfort in artificially ventilated children. Pediatrics 2008; 122(4): e848–53.
27. Aslanidis T, Grosomanidis V, Karakoulas K, Chatzisotiriou A. Electrodermal activity monitoring during endotracheal sunction in sedated adult Intensive Care Unit patients. Folia Med 2018; 60(1): 92–101.
28. Aslanidis T, Grosomanidis V, Karakoulas K, Chatzisotiriou A. Electrodermal activity monitoring during blood pooling for arterial blood gases analysis in sedated adult Intensive Care Unit patients. Medical Sciences 2018; 6(1): 20.
29. Aslanidis T. Perspectives of Autonomic nervous system perioperative monitoring –focus on selected tools. Int Arch Med 2015; 8(22): 1–9.
30. Doberenz S, Roth WT, Maslowski NI, Wollburg E, Kim S. Methodological Considerations in Ambulatory Skin Conductance Monitoring. Int J Psychophysiology. 2011; 80(2): 87–95.

Severe Hypocalcemia and Extreme Elevation of Serum Creatinkinase in a 16-Year Old Boy with Pseudohypoparathyroidism Type Ib

Štěpán Kutílek[1,2,3,*], Ivana Plášilová[1,3], Kristýna Hasenöhrlová[1], Hana Černá[1], Kristýna Hanulíková[1]

ABSTRACT

Calcium is essential for proper muscular function and metabolism. Myopathy with high creatinkinase activity can be a rare manifestation of hypocalcemia of various origin, such as vitamin D deficiency, hypoparathyroidism, pseudohypoparathyroidism (PHP). 16-year old previously healthy boy was admitted to intensive care unit with convulsions lasting for three minutes and a transient loss of consciousness. Laboratory results revealed severe hypocalcemia (total S-Ca < 1.0 mmol/L; normal 2.2–2.6 mmol/L), hyperphosphatemia (S-P 2.8 mmol/L; normal 0.6–1.6 mmol/L). Serum creatinkinase (S-CK) activity was 32 μkat/L (normal 0.57–2.45 μkat/L). Other basic biochemical parameters including creatinine, troponin, alkaline phosphatase were within normal values. Calcemia was gradually corrected within two weeks by intravenously and orally administered calcium and by cholecalciferol. S-CK reached a maximum of 222 μkat/L on day 4 and dropped to 7.2 μkat/L on day 14. Boy had no myalgias, neither clinical signs of myopathy. Echocardiography was normal with normal myocardial contractility, without any signs of calcification. The serum level of parathyroid hormone (S-PTH) was high (12 pmol/L; normal 0.7–5.5 pmol/L), fully compatible with the diagnosis of PHP. Molecular analysis revealed pseudohypoparathyroidism type Ib (PHPIb).In conclusion, manifest tetany and even mild myopathy with very high S-CK can occur in hypocalcemic patients and usually resolves after normalization of hypocalcemia.

AUTHOR AFFILIATIONS

[1] Department of Pediatrics, Pardubice Hospital, Czech Republic
[2] Department of Pediatrics, Klatovy Hospital, Czech Republic
[3] Department of Pediatrics, Hradec Králové Faculty Hospital and Medical Faculty, Charles University, Czech Republic
* Corresponding author: Department of Pediatrics, Klatovy Hospital, Plzeňská 929, 33901 Klatovy, Czech Republic; e-mail: kutilek@nemkt.cz

INTRODUCTION

Calcium is essential for proper muscular function, muscle contraction and metabolism. Myopathy with high creatinkinase activity (S-CK) can be a rare manifestation of hypocalcemia of various origin, such as vitamin D deficiency, hypoparathyroidism, pseudohypoparathyroidism (1–14).

CASE REPORT

A 16-year old previously healthy boy with uneventful personal history and normal anthropometric data (height 172 cm i.e. 25–50 percentile), weight 64 kg i.e. 50–75 percentile) was admitted to intensive care unit due to convulsions lasting for three minutes and a concomitant loss of consciousness. Upon admission, he was already vigile; Glasgow coma scale (GCS) was 12 points, with positive Chvostek's sign. Laboratory results revealed severe hypocalcemia (total S-Ca < 1.0 mmol/L; normal 2.2–2.6 mmol/L; ionised serum calcium, S-Ca2+ 0.56 mmol/L; normal 1.12–1.23 mmol/L) (Figure 1a,b), hyperphosphatemia (S-P 2.8 mmol/L; normal 0.6–1.6 mmol/L), mild hypomagnesemia (S-Mg 0.64 mmol/L; normal 0.7–1.0 mmol/L). Total serum creatinkinase (S-CK) activity was 32 µkat/L (normal 0.57–2.45 µkat/L). Capillary blood pH was normal (pH 7.388 and 7.424, respectively). Other basic biochemical parameters (serum sodium, potassium, chloride, creatinine, urea nitrogen, troponin and glucose levels, serum activity of aspartate-aminotransferase, alanin-aminotransferase, alkaline phosphatase – S-ALP) were within normal reference ranges. Urinary calcium/creatinine ratio (U-Ca/U-creat) was initially low (0.01 mmol/L:mmol/L; normal 0.1–0.5) (Figure 1c). Urinary dipstick test, including hemoglobin and myoglobin was negative. He immediately received intravenous (i.v.) infusion of 5% dextrose with 10% calcium gluconate and magnesium sulphate. His total calcemia improved within five hours to 1.25 mmol/L (Figure 1a), and S-Mg to 0.88 mmol/L, but S-CK further increased to 38 µkat/L (Figure 2). The following day he received oral calcium (3000 mg/day) and oral cholecalciferol (20,000 IU/day) together with i.v. calcium gluconate. There was a gradual improvement in S-Ca, reaching 1.9 mmol/L on day 14 (Figure 1a). There was a slow gradual decrease in S-P (Figure 1d). However, initially high S-CK was further on rise and began to drop on day 6 (Figure 2). The patient had no myalgias, neither clinical signs of myopathy. There was initially prolonged QTc interval of 0.47 seconds on electrocardiogram, without any signs of myocardial damage, this was normalised on day 14 (QTc 0.42 seconds). Echocardiography was normal with normal myocardial contractility, without any signs of calcification. Abdominal ultrasonography revealed nephrocalcinosis without any signs of urolithiasis. Basal ganglia calcifications were apparent on the magnetic resonance imaging (MRI) of the brain. Patient had no cataract on opthalmological exam. Lumbar spine bone mineral density (L1-L4 BMD) was within age-related reference range (1.188 g/cm2; 0.4 SD Z-score). As mentioned before, the serum levels of creatinine and ALP were normal (66 µmol/L and 2.2 µkat/L, respectively). The wrist X-ray was normal, without any signs

of osteomalacia. The serum level of parathyroid hormone (S-PTH) was high (10.3 and 12 pmol/L, respectively; normal 0.7–5.5 pmol/L). These findings ruled out vitamin D deficiency, chronic renal failure and hypoparathyroidism and were fully compatible with the diagnosis of pseudohypoparathyroidism (PHP). The boy was discharged on day 14 and remained thereafter on calcium (2000 mg/day) and vitamin D supplementation (cholecalciferol 20,000 IU/day, calcitriol 0.25 µg/day). Currently, he is 21 years old, on calcium and vitamin D (cholecalciferol and calcitriol) supplementation with S-Ca 2.2–2.3 mmol/L, no further convulsions occurred. His parents had normal levels of S-Ca, P, ALP, PTH. His brother, who is five years his senior, had asymptomatic hypocalcemia (total S-Ca 1.4 mmol/L) and high S-PTH (14 pmol/L), also confirming the diagnosis of PHP. Therefore, he was also started on calcium and vitamin D supplementation.

Mutational analysis of GNAS gene by Multiple-Ligation Probe amplification revealed deletion of exons STX 16-5 and STX 16-6 together with methylation loss of alternative promotor GNAS1A in both brothers, thus arriving at the diagnosis of pseudohypoparathyroidism type Ib (PHPIb). Mutation of GNAS gene was not detected, confirming diagnosis of PHP Ib.

DISCUSSION

Pseudohypoparathyroidism is a receptor disorder, an end-organ resistance to biological actions of PTH, resulting in hypocalcemia and hyperphosphatemia (15–17). Pseudohypoparathyroidism is caused by genetic defects of GNAS gene, encoding the alpha-subunit of the stimulatory G protein (Gsalpha), a signaling protein essential for the actions of PTH. Pseudohypoparathyroidism is further classified into two main types PHP-I and PHP-II. In PHP-I, both nephrogenous cAMP generation and phosphate excretion following exogenous PTH administration are low compared to those observed in normal subjects. Two principal subtypes of PHP-I have been defined: PHP-Ia and PHP-Ib. Patients with PHP-Ia have, besides PTH-resistance, Albright's hereditary osteodystrophy (AHO), a combination of physical features, such as obesity, short stature, soft tissue calcifications, brachydactyly and mental retardation, together with additional hormonal abnormalities, including hypothyroidism and hypogonadism caused by end organ resistance to thyroid-stimulating hormone (TSH) and gonadotropins (15). Pseudohypoparathyroidism Ib is caused by epigenetic changes at one or multiple differentially methylated regions within GNAS and is therefore characterized by end organ resistance to biological effects of PTH, mostly without dysmorphic features. However, resistance to other hormones and variable features of AHO can also occur (15–17). In PHP-II, nephrogenous cAMP generation is normal, but the urinary excretion of phosphate is impaired. The treatment is currently the same for patients with either PHP-Ia,b or PHP-II and includes calcium supplementation and administration of vitamin D (15). In 2016 the EuroPHP network developed a new classification to include all disorders with impairments in PTH and/or PTHrP signalling pathway, and these have been grouped
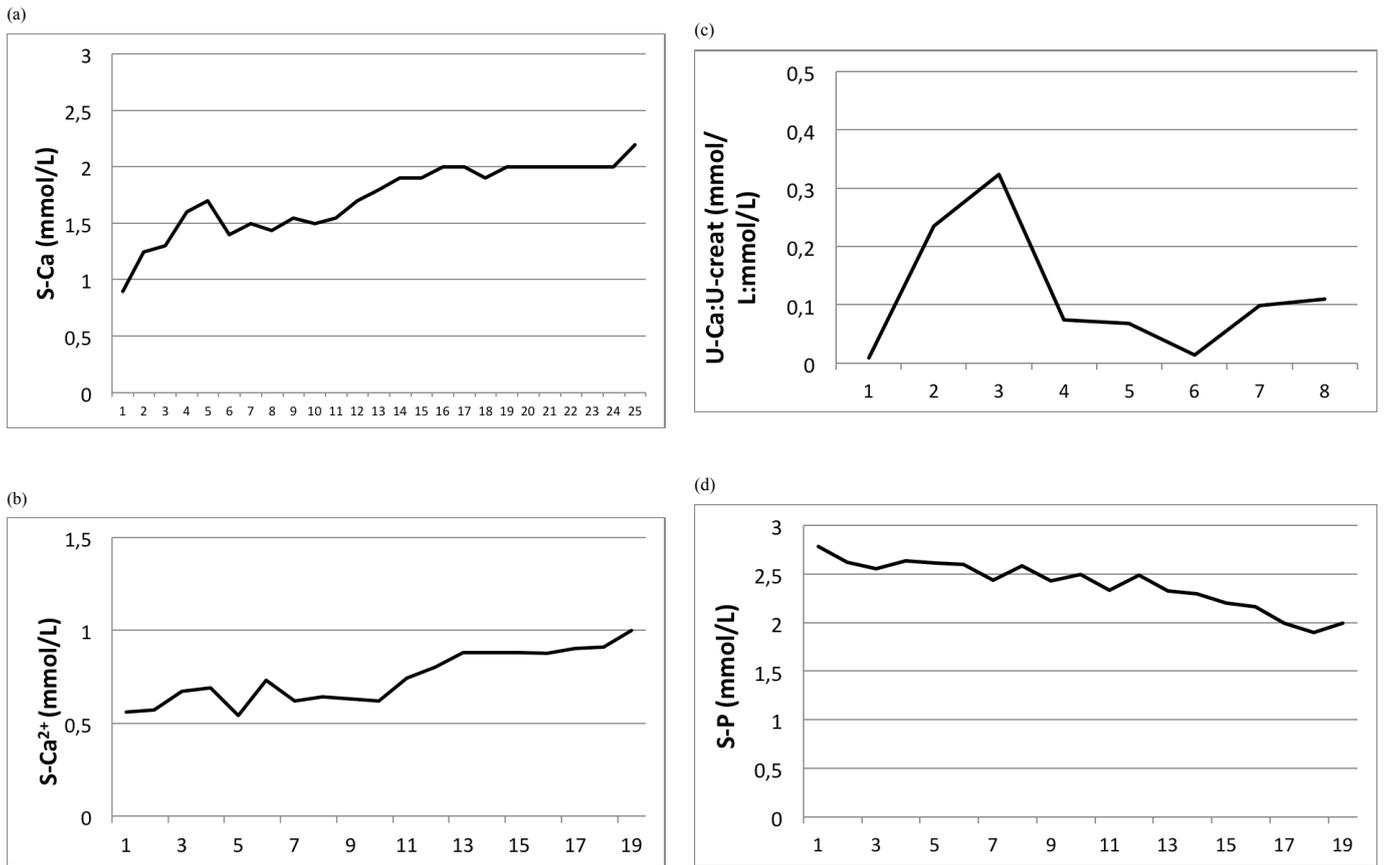
(a)

(c)

(b)

(d)

Fig. 1 (a) Total calcemia (S-Ca; mmol/L) on a daily basis (reference values 2.2–2.6 mmol/L); (b) Ionised serum calcium levels (S-Ca2+; mmol/L) on a daily basis (reference values 1.12–1.23 mmol/L); (c) Urinary calcium/creatinine ratio levels (U-Ca: U-creatinine; mmol/L: mmol/L) on a daily basis (reference values 0.1–0.5 mmol/L); (d) Serum phosphate levels (S-P; mmol/L) on a daily basis (reference values 0.6–1.6 mmol/L).
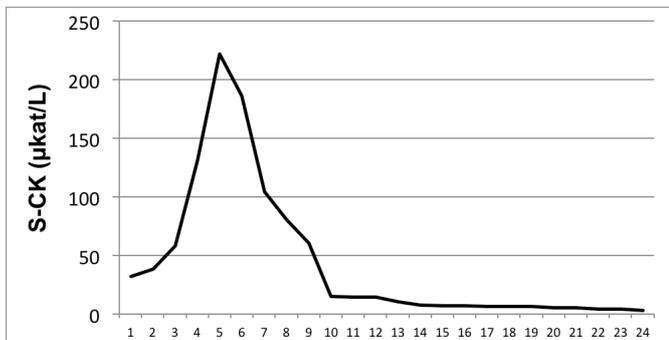

Fig. 2 S-creatinkinase (S-CK, μkat/L) on a daily basis (reference values 0.57–2.45 μkat/L).

under the term "inactivating PTH/PTHrP signalling disorder (iPPSD)" (16, 17).

Several observations reported S-CK elevation in children and adults with hypocalcemia mostly due to hypoparathyroidism (5–10) or PHP (11–14). The mechanism has not yet been elucidated and high S-CK values are believed to be probably the result of rhabdomyolysis or repeated muscle contractions in tetanic seizures (2–5). In another study, microscopic evaluation of bioptic samples revealed muscle cells vacuolar degeneration, focal hyaline degeneration and multiple focal muscle fiber hyaline degeneration with sarcolemma cells hyperplasia in patients with hypoparathyroidism and chronic hypocalcemia (8).

Hypocalcemia may even lead to cardiac arrhytmias (18) and heart failure (19–22). Furthermore, cardiomyopathy with cardiac failure has been reported in patients with hypocalcemia (19, 20).

Our patient presented with severe hypocalcemia due to PHP-Ib, manifest tetany, transiently elevated S-CK with normal cardiac function and without severe myopathy. We did not assess the vitamin D status of this patient at the time of admission, however, normal S-ALP, high S-P together with normal wrist X-ray clearly ruled out vitamin D deficiency.

CONCLUSION

Manifest tetany and even mild myopathy with very high S-CK can occur in hypocalcemic patients and usually resolves after normalization of hypocalcemia.

ACKNOWLEDGEMENTS

This case report was presented as an abstract at the American Society for Bone and Mineral Research (ASBMR) in Baltimore, Maryland, USA, October 4–7, 2013.

REFERENCES

1. Timms P, Bold AM, Rothe P, Lau E. Severe hypocalcemia and increased creatine kinase activity. Br Med J 1985; 291: 937–8.
2. Ishikawa T, Saito M, Morishita H, Watanabe I. Effect of hypocalcemia on muscle in disorders of calcium metabolism. Acta Paediatr Jpn 1995; 37: 367–9.
3. Ishikawa T, Kanayama M, Oba T, Horie T. Hypocalcemic induced increase in creatine kinase in rats. Pediatr Neurol 1998; 18: 326–30.
4. Hirata D, Nagashima T, Saito S, Okazaki H, Kano S, Minota S. Elevated muscle enzymes in a patient with severe hypocalcemia mimicking polymyositis. Mod Rheumatol 2002; 12: 186–9.
5. Ishikawa T, Inagaki H, Kanayama M, Manzai T. Hypocalcemic hyper-CK-emia in hypoparathyroidism. Brain Dev 1990; 12: 249–52.
6. Barber J, Butler RC, Davie MW, Sewry CA. Hypoparathyroidism presenting as myopathy with raised creatine kinase. Rheumatology (Oxford) 2001; 40: 1417–8.
7. Nora DB, Fricke D, Becker J, Gomes I. Hypocalcemic myopathy without tetany due to idiopathic hypoparathyroidism: case report. Arq Neuropsiquiatr 2004; 62: 154–7.
8. Dai CL, Sun ZJ, Zhang X, Qiu MC. Elevated muscle enzymes and muscle biopsy in idiopathic hypoparathyroidism patients. J Endocrinol Invest 2012; 35: 286–9.
9. Cheema UY, Vogler CN, Thompson J, Sattovia SL, Vallurupalli S. Protracted hypocalcemia following post-thyroidectomy lumbar rhabdomyolysis secondary to evolving hypoparathyroidism. Ear Nose Throat J 2015; 94: 113–6.
10. Policepatil SM, Caplan RH, Dolan M. Hypocalcemic myopathy secondary to hypoparathyroidism. WMJ 2012; 111: 173–5.
11. Millichap JG. Friedreich's ataxia forme fruste and elevated creatine phosphokinase in a child with pseudohypoparathyroidism. Childs Brain 1980; 6: 170–4.
12. Piechowiak H, Gröbner W, Kremer H, Pongratz D, Schaub J. Pseudohypoparathyroidism and hypocalcemic "myopathy". A case report. Klin Wochenschr 1981; 59: 1195–9.
13. Gabriel M, Heidemann PH. Elevated creatine phosphokinase activity in pseudohypoparathyroidism. Monatsschr Kinderheilkd 1982; 130: 239–40.
14. Nagasaki K, Tsuchiya S, Saitoh A, Ogata T, Fukami M. Neuromuscular symptoms in a patient with familial pseudohypoparathyroidism type Ib diagnosed by methylation-specific multiplex ligation-dependent probe amplification. Endocr J 2013; 60: 231–6.
15. Bastepe M, Jüppner H. GNAS Locus and Pseudohypoparathyroidism. Horm Res 2005; 63: 65–7.
16. Thiele S, Mantovani G, Barlier A, et al. From pseudohypoparathyroidism to inactivating PTH/PTHrP signalling disorder (iPPSD), a novel classification proposed by the EuroPHP network. Eur J Endocrinol 2016; 175: P1–P17.
17. Takatani R, Molinaro A, Grigelioniene G, et al. Analysis of Multiple Families With Single Individuals Affected by Pseudohypoparathyroidism Type Ib (PHP1B) Reveals Only One Novel Maternally Inherited GNAS Deletion. J Bone Miner Res 2016; 31: 796–805.
18. Isikay S, Akdemir O, Yilmaz K. Pseudohypoparathyroidism presenting with ventricular arrhythmia: a case report. J Clin Res Pediatr Endocrinol 2012; 4: 42–4.
19. Kudoh C, Tanaka S, Marusaki S, et al. Cardiomyopathy in a patient with idiopathic hypoparathyroidism. Intern Med 1992; 31: 561–8.
20. Fisher NG, Armitage A, McGonigle RJ, Gilbert TJ. Hypocalcaemic cardiomyopathy; the relationship between myocardial damage, left ventricular function, calcium and ECG changes in a patient with idiopathic hypocalcaemia. Eur J Heart Fail 2001; 3: 373–6.
21. Rallidis LS, Gregoropoulos PP, Papasteriadis EG. A case of severe hypocalcaemia mimicking myocardial infarction. Int J Cardiol 1997; 61: 89–91.
22. Mavroudis K, Aloumanis K, Stamatis P, Antonakoudis G, Kifnidis K, Antonakoudis C. Irreversible end-stage heart failure in a young patient due to severe chronic hypocalcemia associated with primary hypoparathyroidism and celiac disease. Clin Cardiol 2010; 33: E72–5.

A Long-Term Control of Intramedullary Thoracic Spinal Cord Metastasis from Small Cell Lung Cancer

Hajime Osawa, Shinichiro Okauchi, Gen Ohara, Katsunori Kagohashi, Hiroaki Satoh*

ABSTRACT

Radiotherapy with systemic corticosteroid therapy has been used to treat intramedullary spinal cord metastasis (ISCM), but recovery of function and long-term survival of these patients has been rarely observed. We report herein a small cell lung cancer (SCLC) patient with recurrent thoracic ISCM, who was successfully treated with radiotherapy and systemic corticosteroid therapy. A 70-year-old man, who was diagnosed as having SCLC seven months previously, developed thoracic ISCM. Soon after the detection of the lesion, the patient received radiotherapy with systemic corticosteroid therapy. Sensory disturbance in both extremities and neurogenic bladder and bowel dysfunction was recovered. The patient could walk after irradiation again. The patient received additional chemotherapy and survived 20 months after the diagnosis of ISCM recurrence. Prompt diagnosis and appropriate treatment for ISCM and effective chemotherapy for recurrent SCLC might be the favorable factors for such patients. Further studies will be required to define a favorable subset of patients most likely to benefit from a conventional approach.

AUTHOR AFFILIATIONS

Division of Respiratory Medicine, Mito Medical Center, University of Tsukuba

* Corresponding author: Division of Respiratory Medicine, Mito Medical Center, University of Tsukuba, Miya-machi 3-2-7, Mito, 305-8575, Ibaraki, Japan; e-mail: hirosato@md.tsukuba.ac.jp

INTRODUCTION

Intramedullary spinal cord metastasis (ISCM) is a rare but dismal metastasis, and it has been reported in 0.9–2.1% of all neoplasm autopsies (1–4). Lung and breast carcinomas comprise the most common primary tumor sites in ISCM. Among them, small cell lung cancer (SCLC) is the most common histological type that develop ISCM (3, 5, 6). ISCM is not only associated with severe pain, but also with paralysis, sensory loss, urinary and fecal incontinency, i.e. neurogenic bladder and bowel dysfunction (7–9), when the neurologic elements are compressed. Many patients with intramedullary metastasis whose treatment is not successful suffer from these symptoms that obviously degrade the quality of life. If appropriate treatment cannot be made in time, neuropathy is irreversible even if metastatic lesions shrink. At present, ISCM lacks well-defined treatment guidelines, but rapid diagnosis and appropriate treatment can improve both the quality and length of remaining life. Surgically resectable patients are rare, and irradiation of the metastatic lesion and corticosteroid therapy are usually carried out. Unfortunately, however, complete relief of the symptoms and improvements upon radiological evaluations are rarely expected. Overall prognosis of patients with ISCM is poor (1–3), although a multimodality approach may contribute to the improvement of quality of life and survival.

We show herein a SCLC patient with thoracic ISCM who was successfully treated with a combination of radiotherapy, corticosteroids, and chemotherapy. He experienced relief of the symptoms and showed improvements upon subsequent radiological evaluations. The patient survived 20 months after the diagnosis of ISCM recurrence.

CASE REPORT

A 70-year-old man was admitted to our hospital with weakness and dysesthesia of the bilateral lower extremities, and urinary and fecal incontinence. He was a current smoker. Seven months previously, he was diagnosed as having SCLC in the lower lobe of the left lung (Figure 1). As there was no distant metastasis, he received platinum-containing chemoradiotherapy. Two months after the therapy, he noticed weakness and dysesthesia in left lower extremity, which was rapidly progressing to both lower extremities. Urinary and fecal incontinence was gradually progressed over a month. On admission to our hospital, he was unable to walk. Magnetic resonance imaging (MRI) revealed thoracic ISCM at Th11 (Figure 2-A). Weakness and dysesthesia in both lower extremities, and urinary and fecal incontinence, which was diagnosed as neurogenic bladder and bowel dysfunction, were symptoms due to intramedullary metastasis. As the primary lesion was controlled and no other metastatic site was found, therapy for the ISCM could be started soon after the detection of the ISCM. The patient was treated with dexamethasone at an initial dose of 8 mg per day for 14 days followed by gradual tapering off over the next 2 weeks.
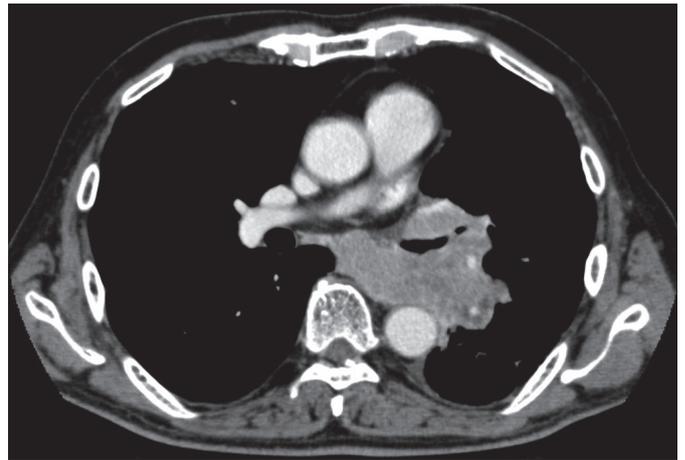

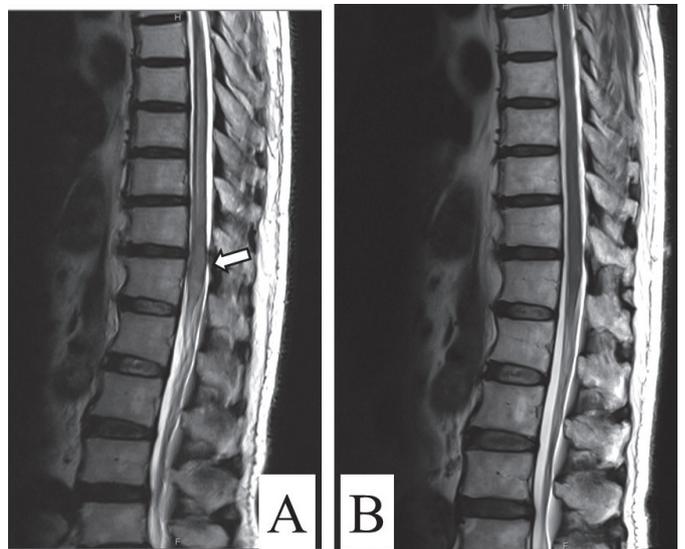**Fig. 1** Chest CT scan at the time of diagnosis of small cell lung cancer.

Fig. 2 Magnetic resonance imaging (MRI) of the thoracic spinal intramedullary metastasis. An intramedullary spinal cord tumor with adjacent edema can be observed at the Th11 level on a T2-weighted image (arrow) (A). The follow-up MRI 2 months after the initiation of irradiation showed a disappearance of the intramedullary spinal cord tumor and adjacent edema at the Th11 level on a T2-weighted image (B).

He received palliative irradiation for the ISCM lesion up to 40 Gy (16 fractions). At the follow-up 3 weeks after the initiation of dexamethasone and radiotherapy, the neurologic status showed distinct improvement insofar as the patient was able to walk a short distance on his own. Improvement of urinary and fecal incontinence was also observed. The follow-up MRI 2 months after the initiation of irradiation showed a significant decrease in the size of the ISCM (Figure 2-B). Thereafter, the patient received 6 courses of platinum-containing chemotherapy, 5 courses of amrubicin, and 2 courses of irinotecan therapy. He was regularly monitored in our outpatient division. He could walk for 18 months but died of SCLC 20 months after the diagnosis of ISCM recurrence.

DISCUSSION

With early diagnosis and appropriate treatment, selected patients with ISCM may benefit from improved neurological outcome and long-term survival, as observed in the present case. In most patients with ISCM, however, treatment is not successful, and they suffer from the symptoms that obviously degrade the quality of life. Even effective, treatment delay can lead to irreversible neuropathy. An unfavorably clinical course in most patients leads to debilitating and disastrous outcomes. Therefore, ISCM is a medical emergency with potentially debilitating and disastrous outcomes (10).

Immediate treatment with irradiation of the ISCM and corticosteroid therapy is the most commonly used option (1–4, 11). Hashii et al reported that 56% of the patients who received radiotherapy showed either neurological improvement or pain alleviation (12). However, other previous reports described that many patients receive these therapies, but rarely with remarkable effect (1–4, 11). In a review by Winkelman (10), clinical evidence for the effectiveness of irradiation of the ISCM and corticosteroid therapy was presented, however, neither shrinkage of the metastatic lesion on MRI nor improvement of impaired symptoms were rarely observed.

Surgery remains the treatment of choice for symptomatic intramedullary lesions, but the optimal management of intramedullary metastasis is still controversial. Despite of recent advances in surgical management of intramedullary metastasis, high complication rate causes clinicians to hesitate to perform surgical resection. Corticosteroids have the effect of reducing edema around the metastatic site. However, no standardized method has been established for the type of administered drug, dosage and administration period. Radiotherapy has an important role, particularly in treatment of radiosensitive tumors and in patients who are not candidates for surgery. Novel approaches such as stereotactic radiosurgery can be promising (13–15). With regard to radiotherapy, standard irradiation method was not established. Recently, stereotactic radiotherapy has attached attention (14, 15). This radiotherapy can be a safe and effective option in selected cases, and is attractive that this radiotherapy may preserve neurological function (14, 15). Radiosensitive tumors may be the most suitable for this radiotherapy.

It is unknown why this patient achieved a good therapeutic effect. The following factors are considered as the reasons of good therapeutic effect. 1) Correct diagnosis was possible within a week from the admission of the patient, though it is difficult to judge onset of ISCM. 2) Multidisciplinary treatments could be started in a week after the detection of the ISCM. 3) At the same time as irradiation, dexamethasone was continued without reducing the dose for 2 weeks. 4) The presence of effective antitumor drugs had important role for long-term control of ISCM.

Since ISCM is debilitating and disastrous metastasis, chest physicians need to be aware of this metastasis. MRI is essential for accurate diagnosis. If there are symptoms suspected of this metastasis, MRI should be performed immediately. Shortening the interval from the appearance of symptoms to the start of treatment is related to the therapeutic effect, though "the prime-time" is beyond our knowledge. To achieve long-term survival, in addition, it is essential to control not only ISCM but also the other lesions than the ISCM. Presence of effective chemotherapeutic drugs is another key factor. Rehabilitation that improves symptoms may also be important. With early diagnosis and appropriate treatment, selected patients can achieve improved neurological outcome and long-term survival. The therapeutic environment in which these multidisciplinary treatments are available and the physical condition of the patient that can withstand these treatments can be circumstances indispensable to achieve successful outcome. It is important to accumulate knowledge and to develop appropriate therapies.

CONFLICT OF INTEREST

None.

FUNDING SOURCE

None.

REFERENCES

1. Costigan DA, Winkelman MD. Intramedullary spinal cord metastasis. A clinicopathological study of 13 cases. J Neurosurg 1985; 62(2): 227–33.
2. Lee SS, Kim MK, Sym SJ, et al. Intramedullary spinal cord metastases: a single-institution experience. J Neurooncol 2007; 84(1): 85–9.
3. Kalayci M, Cagavi F, Gul S, Yenidunya S, Acikgoz B. Intramedullary spinal cord metastases: diagnosis and treatment: an illustrated review. Acta Neurochir (Wien) 2004; 146(12): 1347–54.
4. Okamoto H, Shinkai T, Matsuno Y, et al. Intradural parenchymal involvement in the spinal subarachnoid space associated with primary lung cancer. Cancer 1993; 72(9): 2583–88.
5. Katsenos S, Nikolopoulou M. Intramedullary thoracic spinal metastasis from small-cell lung cancer. Monaldi Arch Chest Dis 2013; 79(3–4): 140–2.
6. Koutsis G, Spengos K, Potagas C, Dimitrakopoulos A, Sfagos K, Zakopoulos N. Intramedullary spinal cord metastases in a patient with small-cell lung cancer. Eur J Intern Med 2006; 17(5): 372–4.
7. Parker AL, Pugh T, Hirsch MA. A rare intramedullary spinal cord metastasis from a retroperitoneal leiomyosarcoma presenting as a non-traumatic spinal cord injury. Am J Phys Med Rehabil 2017; 96(7): e134–7.
8. Fujimoto N, Hiraki A, Ueoka H, et al. Intramedullary spinal cord recurrence after high-dose chemotherapy and autologous peripheral blood progenitor cell transplantation for limited-disease small cell lung cancer. Lung Cancer 2000; 30(2): 145–8.
9. Wilson PE, Oleszek JL, Clayton GH. Pediatric spinal cord tumors and masses. J Spinal Cord Med 2007; 30(Suppl 1): S15–20.
10. Winkelman MD, Adelstein DJ, Karlins NL. Intramedullary spinal cord metastasis. Diagnostic and therapeutic considerations. Arch Neurol 1987; 44(5): 526–31.
11. Hickey M, Farrokhyar F, Deheshi B, Turcotte R, Ghert M. A systematic review and meta-analysis of intralesional versus wide resection for intramedullary grade I chondrosarcoma of the extremities. Ann Surg Oncol 2011; 18(6): 1705–9.
12. Hashii H, Mizumoto M, Kanemoto A, et al. Radiotherapy for patients with symptomatic intramedullary spinal cord metastasis. J Radiat Res 2011; 52(5): 641–55.
13. Mut M, Schiff D, Shaffrey ME. Metastasis to nervous system: spinal epidural and intramedullary metastases. J Neurooncol 2005; 75(1): 43–56.
14. Kaal EC, Vecht CJ. CNS complications of breast cancer: current and emerging treatment options. CNS Drugs 2007; 21(7): 559–79.
15. Hernández-Durán S, Hanft S, Komotar RJ, Manzano GR. The role of stereotactic radiosurgery in the treatment of intramedullary spinal cord neoplasms: a systematic literature review. Neurosurg Rev 2016; 39(2): 175–83.

From Ataxia to Diagnosis of Askin Tumor – a Case Report

Marko Bašković[1,*], Božidar Župančić[1], Mirko Žganjer[1], Igor Nikolić[2], Davor Ježek[3], Lucija Čizmić[4]

ABSTRACT

Peripheral primitive neuroectodermal tumors (pPNET) are a group of extremely rare, aggressive, malignant tumors that are most often found in the thorax (Askin tumor), abdomen, pelvis, extremities and less frequently in the head and neck. The most important prognostic factor is the stage of the tumor. Significant progress both in surgery and in neoadjuvant and adjuvant chemotherapy and radiotherapy, as well as the improvement in diagnosis by cytogenetic and immunohistochemical analysis, should improve the survival rate. We report a case of a 14-year-old girl, with ataxic gait, cardiopulmonary compensated, without respiratory symptoms, who was referred to our hospital for further examination and treatment of newly discovered tumor of the left hemithorax. After a detailed radiological and laboratory investigation, next step was an extensive thoraco-neurosurgical surgery. After histopathological, cytological and molecular analysis, a diagnosis of Askin tumor was made.

AUTHOR AFFILIATIONS

[1] Department of Pediatric Surgery, Children's Hospital Zagreb, Zagreb, Croatia
[2] Department of Thoracic Surgery, Clinical Hospital Dubrava, Zagreb, Croatia
[3] Department of Histology and Embriology, University of Zagreb, School of Medicine, Croatia
[4] University of Zagreb, School of Medicine, Zagreb, Croatia
* Corresponding author: Department of Pediatric Surgery, Children's Hospital Zagreb, Ulica Vjekoslava Klaića 16, Zagreb 10000, Croatia; e-mail: baskovic.marko@gmail.com

INTRODUCTION

Primitive neuroectodermal tumors are groups of highly malignant tumors composed of small round cells of neuroectodermal origin. They show a great variety in clinical manifestations and a great cytological similarity to other small cell tumors, which through the past classification of this tumor group caused a series of controversies. Although Askin's tumor was first described in 1979 (1), only Batsakis et al. (2) the family of primitive neuroectodermal tumors divided into three groups; I. primitive neuroectodermal central nervous system tumor, II. neuroblastoma, III. peripheral primitive neuroectodermal tumor (pPNET – tumors that originate from tissues outside the central and autonomic nervous system). Peripheral primitive neuroectodermal tumors are also classified as part of Ewing's tumor family because they represent different manifestations of the same tumor and have similar genetic changes. Ewing's sarcoma is more common in bones, while peripheral primitive neuroectodermal tumors are more common in soft tissues. Immunohistochemical and cytogenetic studies indicate that these tumors have a common origin (known to share the same reciprocal translocation, most commonly between chromosomes 11 and 22), and therefore peripheral primitive neuroectodermal tumors are divided into the following groups; I. Ewing's sarcoma, II. malignant peripheral primitive neuroectodermal tumors (peripheral neuroepithelioma of bone and soft tissues), III. Askin's tumor (peripheral neuroepithelioma of the thoracopulmonary region), IV. other rare tumors (neuroectodermal tumor, ectomesenchymoma, peripheral medullary epithelioma) (3). Peripheral primitive neuroectodermal tumors have very often aggressive clinical behavior compared to other tumors that originate from small round cells of neuroectodermal origin. They are exceptionally rare with an annual incidence (in the age group from the age of 20 years) of 2.9 patients per million inhabitants. In recent major studies, peripheral primitive neuroectodermal tumors mostly occur in the second decade of life with slightly higher frequency in male populations. There are 4–17% of all soft-tissue tumors in the children's population and dominate in children of white race and Latino Americans origin (4).

CASE REPORT

A 14-year-old girl, born of proper pregnancy and childbirth, normal psychomotor development, regular personal and family anamnesis, came to the local hospital due to fatigue in her legs which appeared ten days ago. During the examination, the girl was afebrile, oriented in time and space, regular speech, cardiopulmonally compensated, without respiratory symptoms, with the asymmetry of the lips and ataxic gait. The thorax was asymmetrical with the protuberance of left hemithorax (Figure 1). The auscultatory finding on the heart was tidy, on the both lungs hearing breathing with the left apical rear silent breathing sound. The walk on the heels and fingers did not work, and she stood up adhering to table. She was unstable in Romberg. In the antigravitational position she had a trembling hand. The tetive muscular reflexes of the lower extremities were extended reflex zones. Skin reflections at all levels were not challenged. Head

CT, abdominal ultrasound and lumbosacral spine x-ray were initiated. Head CT and abdominal ultrasound were tidy while lumbosacral spine x-ray noticed soft tissue shadow of the left hemithorax, followed by initiation of chest x-ray by verifying the large shadow of the left hemithorax that suppressed the mediastinal structure contralaterally and compressed the pulmonary parenchymal caudally (Figure 2). The right lung was free of inflammatory and delayed changes. There was no pleural effusion. In the area of the 5th rib on the left was a visible lytic lesion susceptible to osteolysis. With the diagnosis of neoplasm of uncertain or unknown etiology, the girl was transferred to the Children's Hospital Zagreb for further treatment. It is initiated ECG, echocardiogram, thoracic ultrasound and CT, MR of neuroaxis and complete laboratory findings. The echocardiogram showed a fully accurate finding while the ECG recorded sinusoidal frequency 84/min, vertical electric axis (+92 °), time intervals with repolarization disturbance. The thoracic CT was verified by a large, sharply restricted tumor formation of the left chest extending from the apical to the base at a length of 22 cm (Figure 3a), while spreading the volume of the thorax leading to the thoracic wall protrusion (Figure 3b). The tumor suppressed the mediastinal structures contralaterally without infiltrating them. The left bronchus was shown in the initial part, while it was later covered by tumor formation. Tumor formation was mixed characteristics of the inhomogeneous structure, partially filled with denser fluid content absorption coefficient between 20–30 HU, while in the back was predominantly intercalated with calcifications and fibrous elements. The back part of the fifth rib in the length of 50 mm was destroyed as well as the associated costovertebral joint. MR of neuroaxis at ThIV, ThV and ThVI levels showed intraspinal propagation of tumor of extradural position (Figure 4). Laboratory findings were within normal limits except for the following; sedimentation 75 (↗), lactate dehydrogenase 258 (↗), ferritin 156 (↗), NSE 20.2 (↗). On the third day, ultrasound was performed by percutaneous puncture biopsy through the third intercostal space in the posterior axillary line. The tissue cylinder referred to pathohistological and cytological analysis that did not find tumor cells. On the tenth day, a combined thoraco-neurosurgical surgery was initiated. The surgical procedure involved a left thoracotomy, full extirpation of a huge tumor spreading into the spinal canal, decompression laminectomy (ThIV–ThVI) and the 5th rib resection. The final diagnosis was obtained by a pathohistological, cytological and molecular analysis. The tumor was encapsulated, partly cystic, in a solid part with the necrosis. It was a tumor of small blue round cells constructed of diffuse proliferation of uniform cells of blastoid nuclei, gentle chromatin of scarce cytoplasm, with numerous apoptotic bodies and with 10 mitoses at 10 VF. Immunohistochemical, described tumor cells were vimentin, CD 99, and a smaller portion of NSE positive whereas only CKAE1/AE3, EMA and S100 were positive. The Ki67 proliferation marker was positive in 20% of tumor cells. RT-PCR determined translocation t (11; 22) (q24; q12) EWSR1/FLI1. Multiple times, chest x-ray indicated incomplete reexpand left pulmonary parenchyma which was also expected due to long compression (Figure 5). On the eighth postoperative day, the thoracic drain was replaced by a pleurostomia catheter connected to the Heimlich valve and a chemotherapy treatment with the VIDE (vincristine, ifosfamide, doxorubicin, etoposide) initiated according to EURO-E.W.I.N.G. 99 protocol.
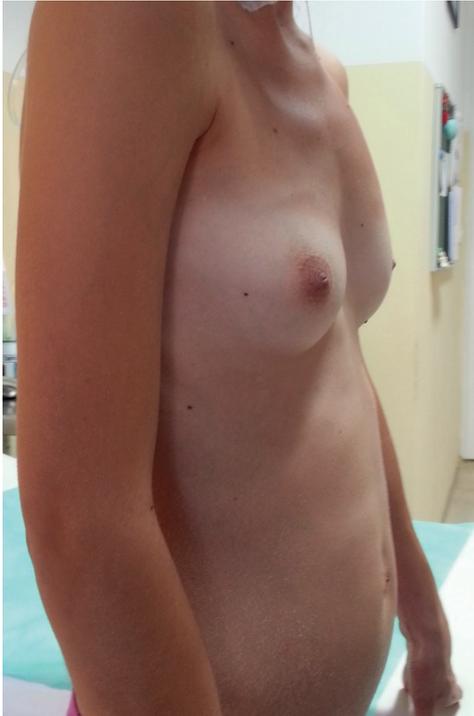
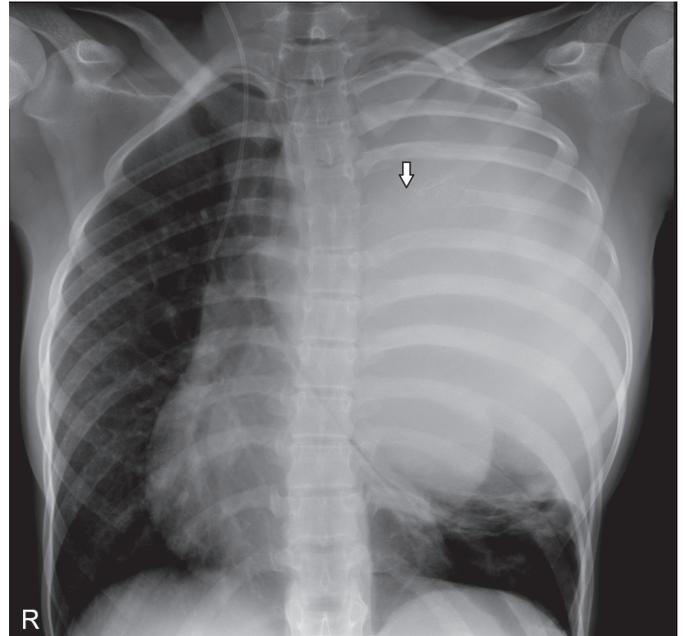**Fig. 1** The patient with discrete prominence left hemithorax.

Fig. 2 Chest x-ray – a large soft tissue shadow of left hemithorax which suppresses mediastinal structures contralaterally and compresses the lung parenchyma caudally with subsequent subsegmental plate atelectasis. Osteolytic lesions of the 5th rib (marked with an arrow).
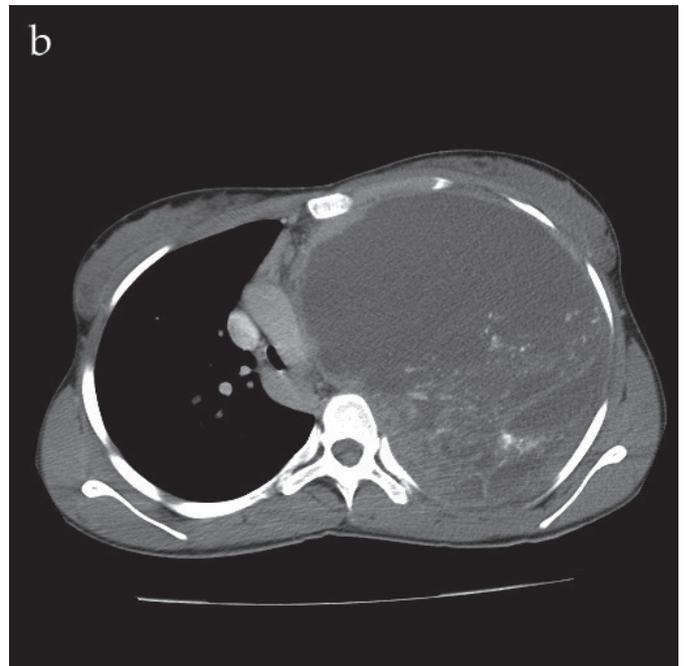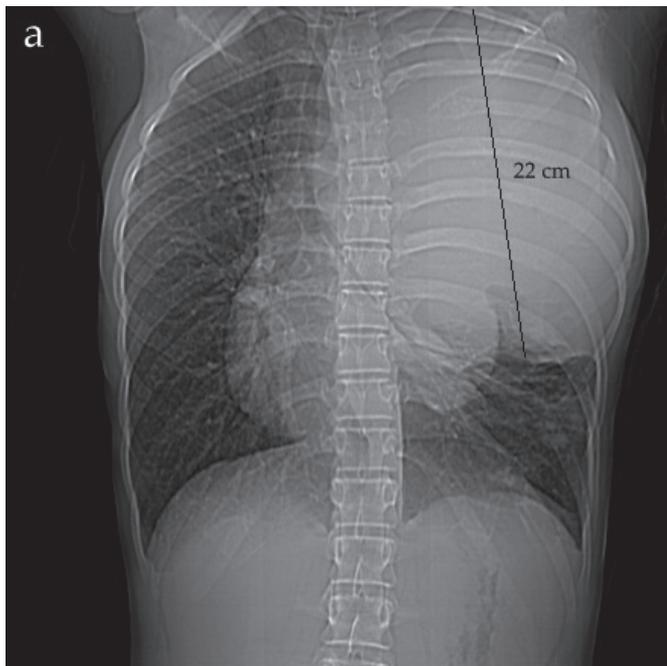

Fig. 3 Thorax CT (a – sharply limited tumor formation of the left chest that extends from the apex to the base in the length of 22 cm; b – transverse cross-section of the thorax showing the forward bulging of the thoracic wall).

DISCUSSION

By reviewing literature, most peripheral primitive neuro-ectodermal tumors are affected by thorax (Askin's tumor), pelvis, abdomen and extremities (5, 6, 7). Thoracic involvement is described in more than sixty cases. Interestingly, in the series of Jones and McGill tumor localization as many as 11 out of 26 patients in the area of the head and neck (8). Clinical symptoms depend on the localization and on the stage of the tumor. It is interesting to note that the patient from our presentation had no symptoms of pain in the chest wall, dyspnea, cough, and weight loss as we can notice in other reports (9, 10). Ataxia, as the leading symptom, has not been recorded in any case so far. Literature as
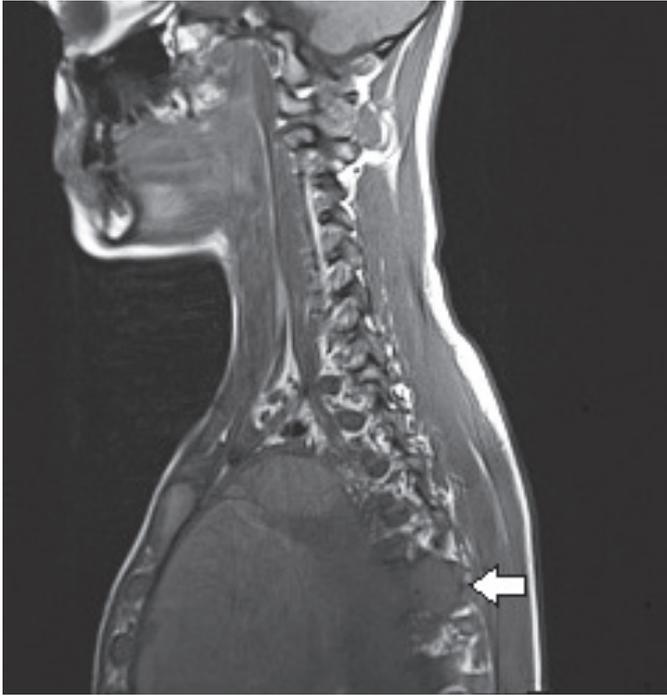
Fig. 4 MR of neuroaxis (sagittal section) – intraspinal propagation of the tumor process at the ThIV, ThV and ThVI level (indicated by the arrow).
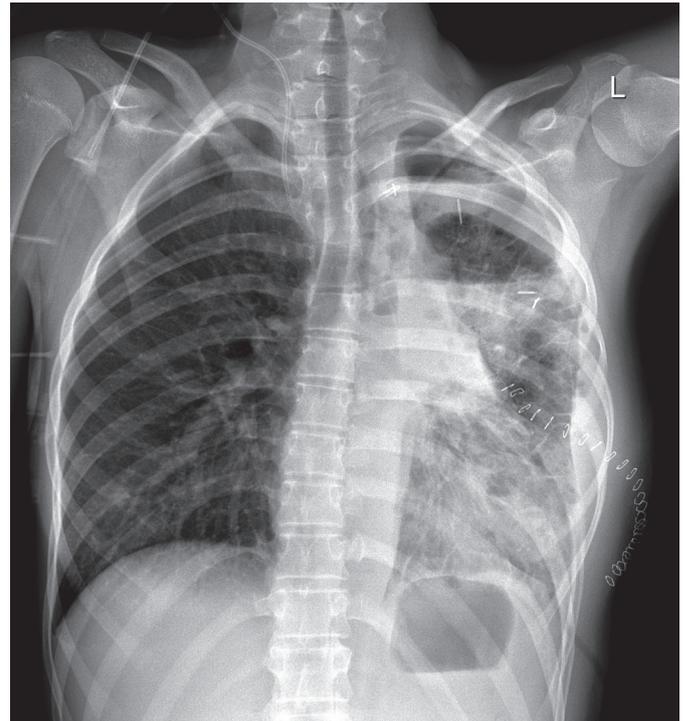

Fig. 5 X-ray of the lungs after the surgery – incomplete reexpansion of the lung parenchyma with resection of the 5th rib.

the leading cause of ataxia states the following conditions; central postinfectious and inflammatory causes, acute postinfectious cerebellar ataxia, postinfectious cerebellitis, ADEM, the clinically isolated syndrome, MS, spinal and peripheral postinfectious and inflammatory causes, Guillaine-Barré syndrome, Miller Fisher syndrome, Bickerstaff brainstem encephalitis, transverse myelitis, toxic ingestion (benzodiazepines, antiepileptics: carbamazepine and phenytoin, cough syrup: dextromethorphan, ethanol, marijuana), childhood stroke, intracranial bleeding, vertebral artery dissection, cerebellar venous infarction, meningitis, rhombencephalitis, labyrinthitis and celiac disease (11). In several large series of metastases, 21–30% of patients (lungs, bones, bone marrow) have been reported. The two-year survival rate is 28–38%, and five-year survival rate is only 14–17% (6, 12).

As far as tumor diagnostics are concerned, data obtained by light microscopy, cytogenetic analysis and immunohistochemical methods are of crucial importance in the definitive diagnosis of Askin's tumor. Based on histological studies alone, it is impossible to distinguish Askin's tumor from e.g. rhabdomyosarcoma, neuroblastoma or mesenchymal chondrosarcoma, where in all cases we find small, round, dark-colored cells. Electron microscopy in peripheral primitive neuroectodermal tumors reveals neurosecretory granules with microtubules and microfilaments. The final diagnosis by which peripheral primitive neuroectodermal tumors are distinguished from other small, round cell tumors and represented by most pathologists and cytologists is based on the immunohistochemical analysis of MIC2 (CD99) gene expression that produces an antigen (13). Recently, the immuno-histochemical analysis of NKX2-2 gene product has become

increasingly important (8). There are other nonspecific markers that are also used in the diagnosis of this tumor group; S-100, vimentin, neuron specific enolase, CD75 and synaptophysin (14).

Radiology, primarily in the form of computerized tomography and magnetic resonance, definitely helps us to determine the limits of the tumor and the presence of metastasis. At CT, peripheral primitive neuroectodermal tumors primarily appear as heterogeneous masses, often infiltrating surrounding tissues. According to Ba et al. these tumors were hypodense, and osteolytic focal points were a sign that the tumor originated from the bone (15). Analogously to our radiological finding Xiao et al. as the main CT characteristics of these tumors described an irregular form (83.3%), heterogeneity (66.7%) and hypodensity (94.4%) (16).

As far as treatment is concerned, current guidelines are in favor of complete surgical resection (17). It is necessary, as far as possible, to completely remove the tumor, although this is not always possible with regard to the infiltration of vital structures. Chemotherapy and radiotherapy (adjuvant and non-adjuvant) are also key in treating this tumor. A review of literature is based on a series of protocols ranging from only two to six chemotherapeutics (18). Combinations used in the largest number of cases are doxorubicin, actinomycin D, cyclophosphamide, ifosfamide, vincristine, etoposide, busulfan, melphalan and carboplatin (VACA – vincristine, doxorubicin, cyclophosphamide, actinomycin, VAIA – vincristine, doxorubicin, ifosfamide, actinomycin, EVAIA – VAIA + etoposide; VIDE – vincristine, ifosfamide, doxorubicin, etoposide) (19). Carvajal and Meyers, with a comprehensive review of chemotherapy protocols and outcomes, recommended

the following regimen; vincristine, doxorubicin and cyclo-phosphamide with ifosfamide and etoposide (20). More recently, the use of adjuvant radiotherapy with doses greater than 60 Gy has been abolished since studies have shown that doses greater than 60 Gy are causing secondary malignancies. Kuttesch et al. reported that 20% of patients who received a dose greater than 60 Gy developed secondary malignant neoplasm (21).

FUNDING

None.

CONFLICTS OF INTEREST

The authors declare that there is no conflict of interest.

REFERENCES

1. Askin FB, Rosai J, Sibley RK, Dehner LP, McAlister WH. Malignant small cell tumor of the thoracopulmonary region in childhood: a distinctive clinicopathologic entity of uncertain histogenesis. Cancer 1979 Jun; 43(6): 2438–51.
2. Batsakis JG, Mackay B, El-Naggar AK. Ewing's sarcoma and peripheral primitive neuroectodermal tumor: an interim report. Ann Otol Rhinol Laryngol 1996 Oct. 105(10): 838–43.
3. Honrado CP, Moscatello AL, Wilson YL, Weissbrod PA. Primitive Neuroectodermal Tumors Medscape 2016; Mar 01.
4. Windfuhr JP. Primitive neuroectodermal tumor of the head and neck: incidence, diagnosis, and management. Ann Otol Rhinol Laryngol 2004 Jul; 113(7): 533–43.
5. Jürgens H, Bier V, Harms D, et al. Malignant peripheral neuroectodermal tumors. A retrospective analysis of 42 patients. Cancer. 1988 Jan 15; 61(2): 349–57.
6. Kushner BH, Hajdu SI, Gulati SC, Erlandson RA, Exelby PR, Lieberman PH. Extracranial primitive neuroectodermal tumors. The Memorial Sloan-Kettering Cancer Center experience. Cancer 1991 Apr 1; 67(7): 1825–9.
7. Marina NM, Etcubanas E, Parham DM, Bowman LC, Green A. Peripheral primitive neuroectodermal tumor (peripheral neuroepithelioma) in children. A review of the St. Jude experience and con-troversies in diagnosis and management. Cancer 1989 Nov 1; 64(9): 1952–60.
8. Jones JE, McGill T. Peripheral primitive neuroectodermal tumors of the head and neck. Arch Otolaryngol Head Neck Surg 1995 Dec; 121(12): 1392–5.
9. Benbrahim Z, Arifi S, Daoudi K, Serraj M, Amara B, et al. Askin's tumor: a case report and literature review. World Journal of Surgical Oncology 2013; 11: 10.
10. Bekić A, Mehulić M, Gorečan M, Kukulj S, Krmpotić D, Veir M. Askin's tumor – a rare tumor of the thoracopulmonary region. Acta Clin Croat 2004; 43: 49–53.
11. Caffarelli M, Kimia AA, Torres AR. Acute Ataxia in Children: A Review of the Differential Diagnosis and Evaluation in the Emergency Department. Pediatr Neurol 2016; 65: 14–30.
12. Contesso G, Llombart-Bosch A, Terrier P, et al. Does malignant small round cell tumor of the thoracopulmonary region (Askin tumor) constitute a clinicopathologic entity? An analysis of 30 cases with immunohistochemical and electron-microscopic support treated at the Institute Gustave Roussy. Cancer 1992 Feb 15; 69(4): 1012–20.
13. Ishii N, Hiraga H, Sawamura Y, Shinohe Y, Nagashima K. Alternative EWS-FLI1 fusion gene and MIC2 expression in peripheral and central primitive neuroectodermal tumors. Neuropathology. 2001 Mar; 21(1): 40–4.
14. Armbruster C, Huber M, Prosch H, Dworan N, Attems J. Ewing's sarcoma and peripheral primitive neuroectodermal tumor in adults: different features of a rare neoplasm. Onkologie 2008 Apr; 31(4): 179–84.
15. Ba L, Tan H, Xiao H, Guan Y, Gao J, Gao X. Radiologic and clinico-pathologic findings of peripheral primitive neuroectodermal tumors. Acta Radiol 2015; 56(7): 820–8.
16. Xiao H, Bao F, Tan H, Wang B, Liu W, Gao J, et al. CT and clinical findings of peripheral primitive neuroectodermal tumour in children. Br J Radiol 2016 Feb 23; 89(1060): 20140450.
17. Veronesi G, Spaggiari L, De Pas T, et al. Preoperative chemotherapy is essential for conservative surgery of Askin tumors. J Thorac Cardiovasc Surg 2003; 125: 428–9.
18. Tazi I, Zafad S, Madani A, Harif M, Quessar A, Benchekroun S. Askin tumor: a case report with literature review. Cancer Radiothérapie 2009; 13: 771–4.
19. Juergens C, Weston C, Lewis I, et al. Safety assessment of intensive induction with vincristine, ifosfamide, doxorubicin, and etoposide (VIDE) in the treatment of Ewing tumors in the EURO-E.W.I.N.G. 99 clinical trial. Pediatr Blood Cancer 2006; 47: 22–9.
20. Carvajal R, Meyers P. Ewing's sarcoma and primitive neuroectodermal family of tumors. Hematol Oncol Clin North Am 2005 Jun; 19(3): 501–25.
21. Kuttesch JF Jr, Wexler LH, Marcus RB, et al. Second malignancies after Ewing's sarcoma: radiation dose-dependency of secondary sarcomas. J Clin Oncol 1996 Oct; 14(10): 2818–25.

Abnormal Communication between Lateral Thoracic Artery and Anterior Circumflex Humeral Artery – a Case Report

Dinesh V. Kumar*, Ramakrisnan Rajprasath, Prasad G. Bhavani

ABSTRACT

Variations in the branching pattern of axillary artery are observed by many anatomists all over the world. A unique bilateral variation in the axillary artery was observed during the routine dissection of the upper limbs on an approximately 65 year old male cadaver. An abnormal communicative channel was observed between lateral thoracic artery and anterior circumflex humeral artery. It passed between the two roots of median nerve. Arterial anomalies in the upper limb are due to defective remodelling of vascular plexus of the upper limb bud during embryogenesis. Knowledge of variations in axillary artery is quintessential for surgeons, radiologists and anaesthesiologists to avoid treacherous complications during procedures.

AUTHOR AFFILIATIONS

Department of Anatomy, Pondicherry Institute of Medical Sciences, Puducherry, India
* Corresponding author: Department of Anatomy, Pondicherry Institute of Medical Sciences, Puducherry – 605014, India; e-mail: dinesh.88560@gmail.com

INTRODUCTION

Axillary artery being the salient blood vessel of the upper limb extends from the outer border of first rib to the lower border of teres major muscle. It is in intimate relationship with the cords of brachial plexus and its branches and enclosed with the axillary sheath. In anatomical position, artery presents a bold convex curve directed upward and laterally. The artery is divided into three parts by pectoralis minor muscle. Three cords of brachial plexus are named according to their relation to the second part of axillary artery.

Superior thoracic artery is the only branch emanating from the first part of axillary artery. It usually anastomoses with internal thoracic and upper intercostal arteries (1). Of the two branches from the second part of axillary artery, thoraco-acromial artery is shorter and divides into acromial, deltoid, clavicular and pectoral branches. Lateral thoracic artery usually arises from the second part of axillary artery and runs along the lateral border of pectoralis minor muscle. It is the major blood supply to the pectoral muscles, subscapularis and serratus anterior. In addition, it supplies the nipple-areolar complex. One of the devastating complications in plastic reconstruction procedures of the breast is necrosis of the nipple-areolar complex which occurs when there is an irreversible lateral thoracic arterial insufficiency (2). Stook et al. (3) classified the arteries arising from the proximal two-thirds of the axillary artery into two classes: "deep arteries" including the lateral thoracic and superior thoracic arteries; and "superficial artery" (thoraco-acromial artery).

Third part of axillary artery gives three branches namely anterior circumflex humeral artery, posterior circumflex humeral artery and subscapular artery. The anterior circumflex humeral artery runs deep to coracobrachialis and both heads of biceps (4). It then participates in anastomoses with posterior circumflex humeral artery. Median nerve which usually lies anterior to axillary artery is formed by the union of medial and lateral roots from medial and lateral cords of brachial plexus respectively. Knowledge of branching pattern in this region is essential for orthopaedic surgeons attempting to reduce old dislocations and fractures (1).

CASE REPORT

During routine dissection of the axilla, a bilateral variation was found in the typical branching pattern in an approximately 65 year old formalin fixed male cadaver. The axillary artery and its branches were identified after clearing the fat. The first two parts of the axillary artery and its branches were normal. The third part of the axillary artery gave three branches as described. Median nerve was formed by medial and lateral roots coming from medial and lateral cords of brachial plexus respectively as routinely described.

    An abnormal arterial trunk (Fig. 1) was given off from the lateral thoracic branch of the second part. It then coursed downwards and laterally (Fig. 2) between the two roots of the median nerve and joined the anterior circum-
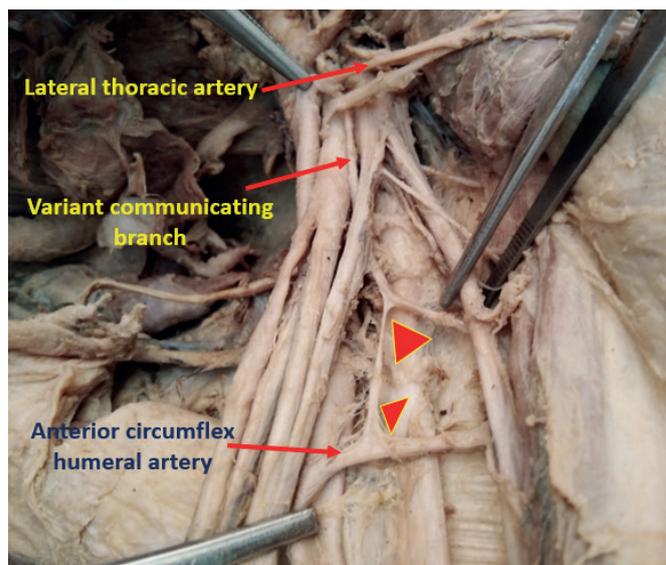

Fig. 1 Dissection of left axilla showing the abnormal communicative vessel (arrow heads) between lateral thoracic artery and anterior circumflex humeral artery. The aberrant vessel passes between the two roots of median nerve.
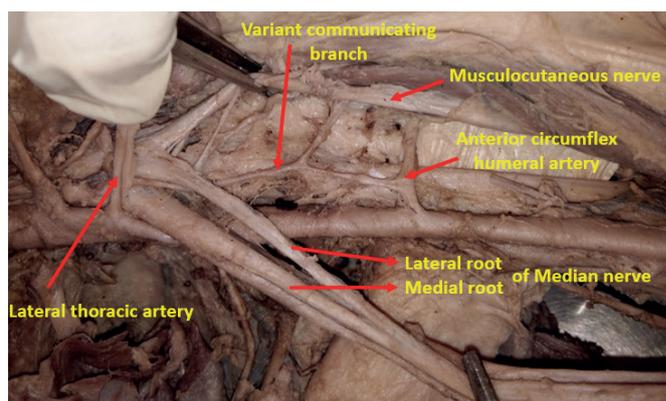

Fig. 2 Course of abnormal communicative channel parallel to axillary artery. A muscular branch can also be noticed emanating from the trunk of aberrant vessel

flex humeral artery of the third part (Fig. 3). The length of the arterial trunk was 5.4 cm and the diameter was found to be smaller than that of lateral thoracic artery. As the trunk was found between the roots of the median nerve, there are chances for it to get compressed. There were no evident signs of stenosis in subclavian, axillary and brachial arteries, which ruled out the possibility of the abnormal trunk being an anastomotic channel. The distribution of other arteries in the upper limb were found to be normal.

DISCUSSION

Earlier studies by many anatomists showed that variations in the upper limb vasculature, particularly in the branching pattern of axillary artery are not so uncommon. In a study (5), it was observed that the normal pattern of distribution is seen in 20% of specimens and the rest
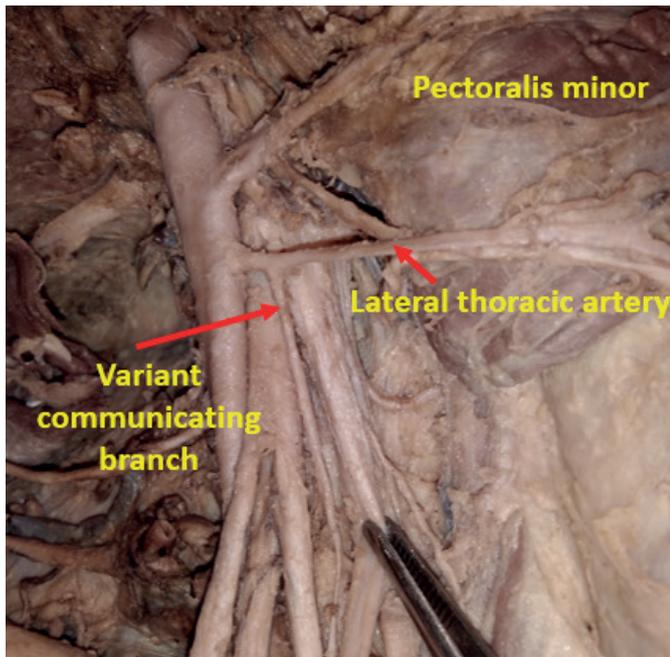
Fig. 3 Proximal portion of aberrant vessel emanating from lateral thoracic artery.

of 80% specimens showed variations in the origin, branching pattern and distribution. In our case report, abnormal communicative channel between lateral thoracic artery and anterior circumflex was observed on both sides.

Studies (6, 7) have documented the common arterial trunk from third part of axillary artery which then divided into branches. Another study (8) documented a common trunk from the second part of axillary artery which then gave origin to thoracoacromial, lateral thoracic, subscapular, and posterior circumflex humeral arteries.

The embryological basis of such abnormal communicative channel might be due to the persistence of communicative channels in the primitive vascular plexus which are usually obliterated during the later stage of embryogenesis (9). Any conditions capable of inducing a regional hypoxia, can also promulgate the formation of such abnormal channels and most of those acquired conditions are mostly unilateral. Any abnormal communication between vessels establishes two circuits in which the blood, flows through two separate systems. One circuit (usually the normal one) characterized by high arterial pressure and high peripheral resistance and the other circuit (abnormal) being shorter and of low arterial pressure.

During the initial phase of embryogenesis, endothelial cells are formed first, and undergo proliferation and coalescence into capillary plexus (10). This capillary plexus then gets remodelled into endothelial tubules and later into blood vessels. Various molecular factors such as VEGFR2 and FGFR1 can maintain endothelial formation (10). Abnormal shear stress can act as an endothelial -inducing mesenchymal transition stimulus, both in development and in adult settings (11). A new vessel formation is triggered by endothelial cell activation and sprouting coordinated with controlled detachment of the surrounding mural cells and sustained by further remodelling of vessel

wall (12). Pre-existing vessel might also split by a process known as "intussusception" giving rise to daughter vessels (13). Quiescent endothelial cells, if triggered by suitable molecular factors, get modified into a "tip cell" which then detaches from the basement membrane and initiates the formation of a vascular branch (13). The tip cells migrate under response of molecular factors such as semaphorins and ephrins. Later lumen gets established and forms a new vessel (14).

The primary arterial trunk of the mammalian forelimb develops from seventh intersegmental artery (15). The axillary arterial plexus gets remodelled into longitudinal trunks and with the formation of brachial plexus; they get united to form the adult structure. The initial capillary plexus enters the upper limb bud at stage 12. This plexus begins to differentiate at stage 13 remodelling process starts in the aorta and continues in a proximal to distal sequence. By stage 15 the differentiation has reached the subclavian and axillary arteries (15). Absence of evident signs of arterial stenosis and bilateralism of the variation ensure its congenital aetiology.

The abnormal communicative channel documented in our report, runs between two roots of median nerve. The possible embryological origin for it might be the eighth or ninth intersegmental arteries. This is in concordance with Yang et al. (16), who had postulated with each instance of segmental artery variation also involved a variation in spatial relationship to the branches of brachial plexus. In worst case scenario, the abnormal vessel can get compressed between the roots of median nerve.

Knowledge regarding the variations in axillary vasculature is critical for the surgeons to perform axillary lymph node clearance or excision biopsy in cases of breast carcinoma, in cases of subclavian artery occlusion, aneurysm of axillary artery and axillary haematoma.

Understanding the variations of humeral arteries helps the plastic surgeons to generate flaps for scar releasing procedures of the head and neck (17). Knowing about the variations in humeral arteries is of significance in vascular injuries after proximal humeral fractures. Anatomy of axillary artery is also of utmost importance in cardiothoracic vascular surgery, as they are one of the cannulation sites for bypass procedures (18).

CONCLUSION

Arterial variations in upper limb are clinically important for the surgeons, anaesthetists, interventional radiologists and orthopaedic surgeons. Here we report an abnormal communicative channel between lateral thoracic artery and anterior circumflex humeral artery. The knowledge of such variations should be disseminated to help the clinicians arriving at an accurate diagnostic interpretation and to plan optimal therapeutic intervention.

CONFLICT OF INTEREST

The authors hereby declare that they have no conflict of interest.

REFERENCES

1. Standring S, editor. Gray's anatomy: the anatomical basis of clinical practice. Forty-first edition. New York: Elsevier Limited, 2016.
2. Van Deventer PV, Page BJ, Graewe FR. The safety of pedicles in breast reduction and mastopexy procedures. Aest Plast Surg 2008; 32: 307–12.
3. Stook FP, Zonnevijlle EDH, Groen GJ. A reappraisal of the blood supply of the pectoralis minor muscle. Clin Anat 1994; 7: 1–9.
4. Sinnatamby CS, Last RJ, editors. Last's anatomy: regional and applied. 12th ed. Edinburgh; New York: Churchill Livingstone/Elsevier, 2011.
5. Thampi SM, Vijayamma KN, Kumar RP. Axillary artery – A study on branching pattern and variations. Journal of Evidence Based Medicine and Healthcare 2017; 4(43): 2619–24.
6. Rao RT, Shetty P, Suresh R. Abnormal branching pattern of the axillary artery and its clinical significance. International Journal of Morphology 2008; 26(2): 389–92.
7. Samuel VP, Vollala S, Nayak S, Rao M, Bolla SR, Pammidi N. A rare variation in the branching pattern of the axillary artery. Indian Journal of Plastic Surgery 2006; 39(2): 222–23.
8. Srimathi T. Abnormal branching pattern of the axillary artery-a case report. Int J Basic Med Sci 2011; 2: 73–6.
9. Arey LB. Developmental Anatomy. In: Development of the arteries. 6th Edition. Philadelphia: W. B. Saunders Co, 1957: 375–7.
10. Dejana E, Hirschi KK, Simons M. The molecular basis of endothelial cell plasticity. Nat Commun 2017; 8: 14361.
11. Ten Dijke P, Egorova AD, Goumans MJ, Poelmann RE, Hierck BP. TGF-beta signalling in endothelial-to-mesenchymal transition: the role of shear stress and primary cilia. Sci Signal 2012 Feb 21; 5(212): pt2.
12. Murakami M. Signaling required for blood vessel maintenance: molecular basis and pathological manifestations. International Journal of Vascular Medicine 2012; Article ID 293641.
13. Carmeliet P and Jain RK. Molecular mechanisms and clinical applications of angiogenesis. Nature 2011; 473(7347): 298–307.
14. Adams RH, Eichmann A. Axon guidance molecules in vascular patterning. Cold Spring Harb Perspect Biol 2010; 2: a001875.
15. Rodríguez-Niedenführ M, Burton GJ, Deu J, Sañudo JR. Development of the arterial pattern in the upper limb of staged human embryos: Normal development and anatomic variations. J Anat 2001; 199(4): 407–17.
16. Yang HJ, Gil YC, Lee HY. Intersegmental origin of the axillary artery and accompanying variation in the brachial plexus. Clin Anat 2009; 22: 586–94.
17. Halmy C, Szetei K, Na'dai Z, et al. Posterior circumflex humeral artery perforator flap (PCHAP-flap) in axillary scar release. Orv Hetil 2009; 150: 603–6.
18. Bonatti J, Coulson AS. The subclavian and axillary arteries as inflow vessel for coronary artery bypass grafts combined experience from three cardiac surgery centres. Heart Surg Forum 2000; 3: 307–12.

Topping Phenomenon with Recurrent Spinal Stenosis and Epidural Fibrosis Prevented with Oxidized Cellulose – a Case Report

Radek Hart*

ABSTRACT

Lumbar spinal stenosis is a condition where the neural structures are compressed in the narrowed spinal canal and often situated only within a single specific segment of the spine, most frequently in the lumbar spine. A case report demonstrates a surgical solution of lumbar spinal stenosis with using oxidized cellulose as a prevention of post-operative adhesions and failed back syndrome. A female patient (68) with a significant pain of the lumbar spine lasting for a number of months due to advanced spondylosis, failing to respond to conservative treatment underwent instrumented, posterolateral fusion of affected segments. The patient re-arrived with pain due to spinal stenosis in another segments after 4 and then after 3 years. We repeatedly performed spinal fusion of the affected segments and applied an anti-adhesive gel to the dural sac and the decompressed nerve roots to prevent the development of post-operative adhesions and the "failed back syndrome". Last surgical solution included mobilisation of the simultaneously constricted dural sac through laminectomy. This time we covered the sac using a haemostat made of oxidized cellulose (Traumacel FAM). After this treatment, the patient was again without significant difficulties.

AUTHOR AFFILIATIONS

Department of Orthopaedics and Traumatology, General Hospital Znojmo, Czech Republic
* Corresponding author: Department of Orthopaedics and Traumatology, General Hospital Znojmo, MUDr. Jana Janského 11, 669 02 Znojmo, Czech Republic; e-mail: radek.hart@nemzn.cz

INTRODUCTION

The pain in the lumbar spine is a very frequent patient complaint seen in consultation rooms of general practitioners and specialists. Lumbar spine disorders hold the second position, after airway diseases, in the frequency of patient visits to first-line physicians and present a high proportion of applications for a disability pension. It is also one of the most frequent causes of incapacity for work because it particularly affects patients of the working age, and with the frequently recurrent pain attacks, the financial cost of treatment of chronic vertebropathy is enormous.

Degenerative diseases of the lumbar spine start to develop in humans often very early – in the second and third decade of life, with intervertebral lumbar discs 4 and 5 being affected most frequently. Often, we observe gradual deterioration in all the segments, typically in the lumbar spine. It is the price paid for walking upright on two legs.

For the lumbar spine, results of treatment are usually not as clear as for the diseases of the majority of other anatomical areas of the locomotor system; they are also accompanied by a higher percentage of complications.The choice of the method of treating the degenerative disease of the lumbar spine still remains controversial. Conservative therapy should always be the method of first choice. It needs to be conducted strictly on an individual basis, in a comprehensive manner, and sufficiently long. Only when it fails, we start considering the eventual indication for the surgery in such a patient. Nowadays, spinal fusion still remains a conventional surgical solution. If correctly indicated, it demonstrably improves the quality of life of patients. To date, no one has demonstrated whether the subsequent degeneration of the adjacent segments ("topping syndrome") is caused by spinal fusion or a natural progression of the degenerative process. When evaluating the overall rate of success, spinal fusion treatment, despite the considerable progress in this field, does not fully achieve the level of effect that we can normally see today following compensation of large joints – particularly those of hip (1).

Lumbar spinal stenosis is a condition where the neural structures are compressed in the narrowed spinal canal. This can be a generalised narrowing and can affect the spine in its entirety or, more often, be situated only within a single specific segment of the spine, which most frequently involves the lumbar spine (2). In terms of etiology, it may be primary – congenital/developmental disease, or, more often, a secondary – acquired disease, which mostly involves a degenerative process. Stenosis of the lumbar spine segment is seen most frequently. It was first described in 1949 by Henk Verbiest (1909–1997), a Dutch neurosurgeon. Depending on the location of the narrowing one can distinguish among (a) spinal stenosis in the strict sense (central stenosis), which affects vertebral foramina / spinal canal as such; (b) lateral (uni-/bilateral) stenosis, which presents the narrowing of lateral recessus; and (c) stenosis of the intervertebral foramen (3).

The increasing quality and availability of imaging lead, along with the growing range of therapeutic alternatives, to spinal stenosis being increasingly diagnosed and treated; gradually, also, it is becoming one of the most frequent indications for surgery of the lumbar spine. Spinal claudication that restricts the walking ability of patients with major central lumbar stenosis who sometimes are able to walk for just a few metres is typical in such individuals. Should comprehensive conservative management in the duration of at least three months not lead to improvements, decompression in the form of (mostly instrumented) laminectomy may provide relief (4, 5).

The resulting post-operative scars and their adhesions to the initially relaxed dural sac may be the cause for the development of the so-called "failed back syndrome", i.e., a gradually emerging relapse of patient's difficulties. This is something that we have been striving to prevent by applying an anti-adhesion gel on the dural sac. Its relatively high price of the preparation and, in particular, as well as supply deficits necessitated a search for alternative solutions. As an option, we began to use resorbable haemostats on the basis of oxidised cellulose (Traumacel FAM). Oxidized cellulose is made from pure, natural cotton using controlled oxidation technology. The material with good flexibility is adaptable and has a fibrous structure allowing easy adjustments and can be easily split to obtain the needed quantity. Oxidized cellulose easily adapts to an uneven or poorly accessible surface and in contact with body fluids it turns into a gel and thus minimizes perioperative and early postoperative blood losses and complications. It is atraumatic and 100% resorbable in the body. The antimicrobial properties against a wide range of microorganism are another advantage of oxidized cellulose. In surgery it is usually used in all areas of stopping diffuse bleeding from resection surfaces of parenchymatous organs muscles or body cavities.

CASE REPORT

A female patient (68) was referred to our department due to a significant pain of the lumbar spine lasting for a number of months, with no radicular symptomatology, failing to respond to conservative treatment. Advanced spondylosis was found in standard X-ray scan, CT and MRI examinations, affecting L3–L4 and L5–S1 segments. Subsequently, we carried out instrumented, posterolateral fusion of these two segments, and, as a preventative measure, stabilised the healthy L4–L5 segment using a flexible interlaminar implant (Fig. 1). The patient was satisfied after this treatment. Four years later, the pain in her lumbar spine reappeared, this time associated with spinal claudications. Functional X-ray images revealed spondylosis and instability of the L4–L5 segment; MRI images also showed a major central stenosis of this segment. Therefore, spinal fusion was performed for the L4–L5 segment as well – PLIF technique was used which simultaneously releases the dural sac in the segment. An anti-adhesive gel was applied to the dural sac and the decompressed nerve roots to prevent the development of post-operative adhesions and the emergence of "failed back syndrome" (Fig. 2). The still healthy segment L2–L3, was treated with a flexible interlaminar implant to avoid the "topping syndrome". Again, the subjective condition of the patient after

this intervention was satisfactory. After three years, however, she re-arrived at our outpatient department with pain, this time in the thoracolumbal segment, and newly developed spinal claudications. Standard X-ray and MRI scans revealed a new degeneration of intervertebral discs in the thoracolumbal junction, with the maximum extent present in the L1–L3 segments where a major central stenosis had also developed (Fig. 3). After consultation with the patient, we extended the transpedicular instrumentation with posterolateral fusion up to T10 (to prevent the frequent "topping syndrome" in the region of the thoracolumbal junction), added S2-iliac screws to ensure four-point fixation of long instrumentation in the sacral region, and mobilised the simultaneously constricted dural sac through laminectomy of the L1–L3 vertebrae (Fig. 4). We covered the sac to prevent post-operative adhesions and the "failed back syndrome", this time using haemostat made of oxidized cellulose (Traumacel FAM Strata

7.5 × 5 cm) (Figs. 5 and 6). After this treatment, the patient is again without significant difficulties. She is now being followed-up for another three years and does not complain of any troubles regarding spinal claudications or nerve root irritation.
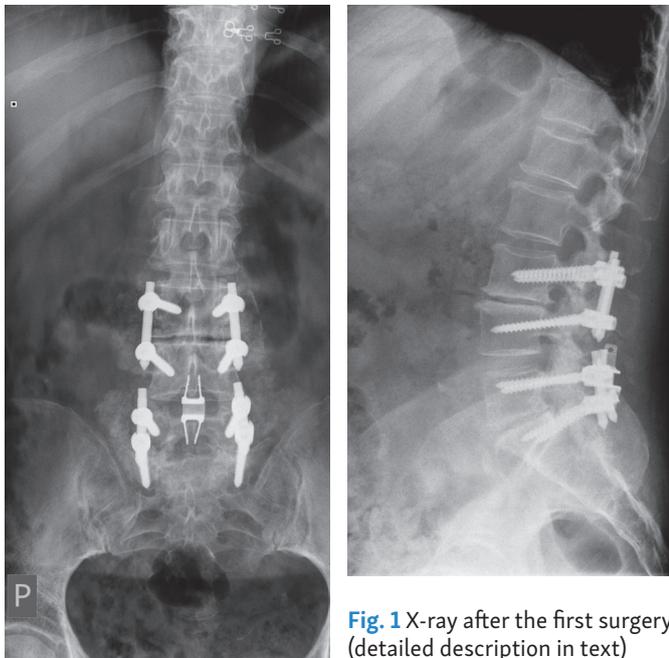

Fig. 3 MRI finding of severe absolute central spinal stenoses L1–L3 before the last surgical intervention.

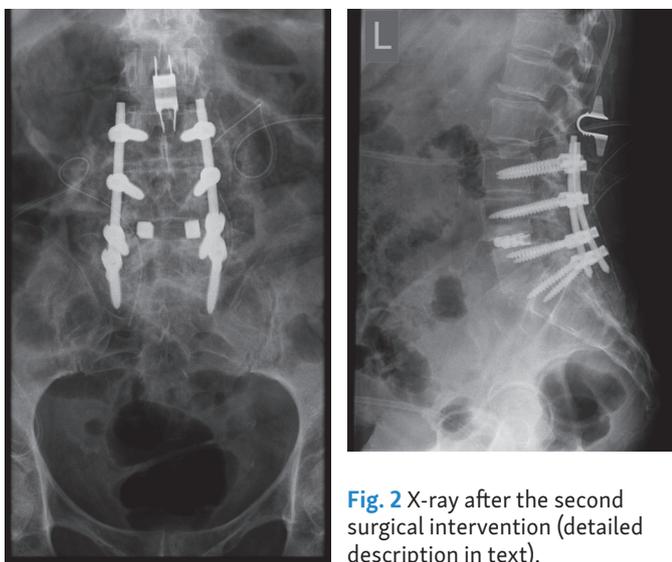**Fig. 1** X-ray after the first surgery (detailed description in text)

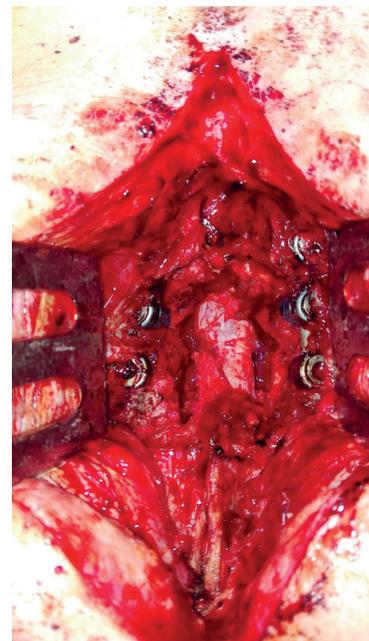**Fig. 2** X-ray after the second surgical intervention (detailed description in text).
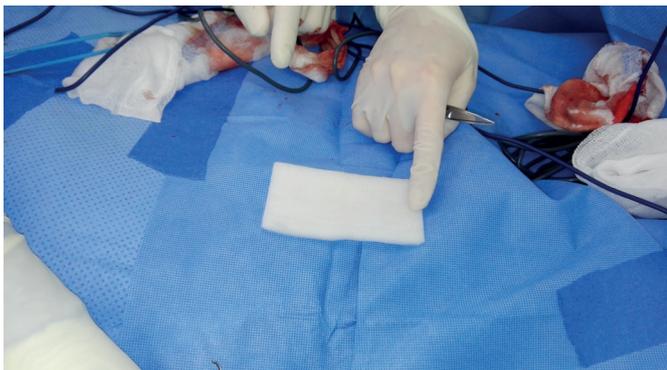

Fig. 4 Decompressed dural sac after laminectomy

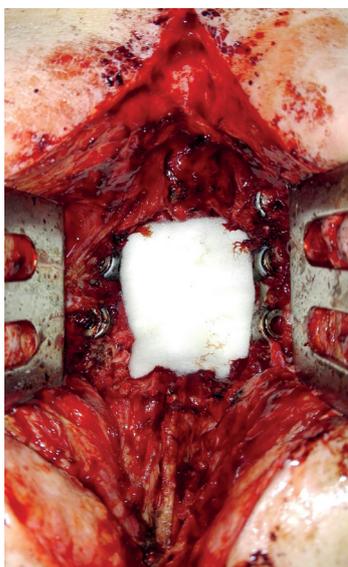Fig. 5 Oxidized cellulose (Traumacel FAM Strata 7.5 × 5cm).

Fig. 6 The cover of the dural sac with a haemostatic agent made of oxidized cellulose Traumacel FAM Strata 7.5 × 5 cm.

DISCUSSION

The development of degenerative changes in the lumbar spine is a very frequent problem in the local population, with a high interindividual variability in the degree of subjective complaints. Any occurring concomitant narrowing of the spinal canal aggravites the condition. For a long time, correlation between the morphological changes and the severity of the spinal claudication was not clear. In spinal stenosis, the discrepancy between the dimensions of the nerve structures and the space available in the spinal canal is the key issue. This causes mechanical compression of both nerve and vascular structures and a complex of typical clinical symptoms. In 1954, Verbiest classified lumbar spinal stenosis, based on the anteroposterior diameter of the spinal canal, as the absolute type, dimension < 10 mm, and the relative type, dimension of 10–14 mm. The main problem with quantifying classification is that the severity of the structural finding does not correlate with that of the clinical finding, i.e., that the degree of compression of the nerve structure is not a factor for the severity of the symptoms, thus not any guide

to indicate a surgical intervention, i.e., decompression. Crucial in this regard was the paper by Barze et al. (Fig. 6) of 2010. Using the so-called "sedimentation sign" in the magnetic resonance imaging (MRI), they managed to distinguish non-specific low back pain from symptomatic lumbar spinal stenosis. In the same year, Schizas et al. (Fig. 7) quantitatively scaled the severity of lumbar spinal stenosis on the basis of the morphology obtained as part of an MRI examination (T2-weighted) with regard to the indication and the prognosis of surgical decompression of the dural sac. In the mildest lumbar spinal stenosis grade (A), there is "free" space in the dural sac around the nerve roots (a negative sedimentation sign). For grade B, nerve roots evenly fill the entire space of the dural sac; there is no "free" liquor around them (a positive sedimentation sign). For grade A and B, surgical solutions are not recommended – conservative treatment is usually sufficient. For grade C, cerebro-spinal fluid is no longer noticeable on MRI and roots are less differentiable; dorsal epidural fat is however still apparent, and the cross-section of the spinal canal has its typical triangular shape. For the most severe grade, D, the cross-section of the spinal canal is so small that neither nerve roots nor epidural fat can be identified. Patients with C/D grade are no longer appropriate to undergo conservative therapy and shall be indicated for surgical treatment.

The decompression of the nerve structure as such is just the first step of the treatment of the spinal stenosis. The second step involves the effort to prevent post-operative adhesions and the "failed back syndrome". For a number of years, application of an anti-adhesive gel was recommended for this purpose; the special gel has been proven to have a positive effect of preventing adhesions. However, new studies are emerging pointing the risks associated with the use of this gel (8). This fact, combined with interruptions in the supplies of the product, led us to the effort to find a different solution. The discussion on this topic is still very limited in the world literature, and published scientific studies (mostly from Turkey) were conducted only on laboratory animals. Some of these works show a significant positive effect of oxidized cellulose on the prevention of epidural fibrosis (9, 10), another a significantly lower effect (11, 12).

CONCLUSION

Our first experience with Traumacel FAM, resorbable haemostat made of oxidised cellulose, as part of preventing dural sac adhesions, is very good. Longer follow-up is necessary to confirm our first results.

REFERENCES

1. Hart R, et al. Degenerativní onemocnění páteře. Praha: Galén, 2014.
2. Delank KS, Fürderer S, Eysel P. Die lumbale Spinalkanalstenose. Z Orthop 2004; 142: 19–35.
3. Schulte TL, Bullmann V, Lerner T, et al. Lumbale Spinalkanalstenose. Orthopäde 2006; 35: 675-94.
4. Yuan PS, Albert TJ. Nonsurgical and surgical management of lumbar spinal stenosis. J Bone Joint Surg Am 2004; 86: 2320-30.
5. Hansraj KK, Cammisa FP, O'Leary PF. Decompressive surgery for typical lumbar spinal stenosis. Clin Orthop 2001; 384: 10–17.

6. Barz T, Melloh M, Staub LP et al. Nerve root sedimentation sign. Evaluation of a new radiological sign in lumbar spinal stenosis. Spine 2010; 35: 892–7.

7. Schizas C, Theumann N, Burn A, et al. Qualitative grading of severity of lumbar spinal stenosis based on the morphology of the dural sac on magnetic resonance images. Spine 2010; 35: 1919–24.

8. Kim SB, Lim YJ. Delayed detected unexpected complication of Adcon-L Gel in lumbar surgery. J Korean Neurosurg Soc 2010; 48: 268–71.

9. Temel SG, Ozturk C, Temiz A, et al. A new material for prevention of epidural fibrosis after laminectomy: oxidized regenerated cellulose (interceed), an absorbable barrier. J Spinal Disord Tech 2006; 19: 270–5.

10. Rodgers KE, Robertson JT, Espinosa T, et al. Reduction of epidural fibrosis in lumbar surgery with Oxiplex adhesion barriers of carboxymethylcellulose and polyethylene oxide. Spine J 2003; 3: 277–83.

11. Altun I. An experimental study of histopathologic effects of hemostatic agents used in spinal surgery. World Neurosurg 2016; 90: 147–53.

12. Karasu H, Güzel I. Comparison TachoComb with SurgiWrap, Surgicel and Lyodura in epidural fibrosis: an experimental rat model. Ideggyogy Sz 2016; 30: 195–200.

Cerebral Infarction in Young Marijuana Smokers – Case Reports

Libor Šimůnek[1,*], Antonín Krajina[2], Roman Herzig[1], Martin Vališ[1]

ABSTRACT

Introduction: Causality of marijuana abuse with development of ischemic stroke has been indicated by numerous case reports and epidemiological studies. As a possible pathophysiological mechanism, the most common consideration is cardiac embolization during paroxysmal atrial fibrillation, systemic hypotension or multifocal intracerebral vasoconstriction. Case reports: We present three case reports of marijuana consumers who were admitted to our comprehensive stroke center due to ischemic stroke within 18-month period of our investigation. In one case, the cause of stroke was not related to the use of marijuana, it was a manifestation of antiphospholipid syndrome. In two cases the association with the abuse of this drug is probable but not certain. In both these cases, an isolated occlusion in vertebrobasilar arterial system was detected, without finding of a cerebral vessels stenosis. Although we did not register the atrial fibrillation, we consider cardiac embolization as probable etiological mechanism of stroke in both cases. In one case, paradoxical embolization due to the persistent foramen ovale represents another potential etiological mechanism. Conclusions: Cannabinoid use may cause ischemic stroke, especially in the younger age category. Therefore, in these patients we recommend focusing on the history of cannabinoid abuse and carry out toxicological urine tests.

AUTHOR AFFILIATIONS

[1] Department of Neurology, Comprehensive Stroke Center, Charles University, Faculty of Medicine and University Hospital, Hradec Králové, Czech Republic

[2] Department of Radiology, Comprehensive Stroke Center, Charles University, Faculty of Medicine and University Hospital, Hradec Králové, Czech Republic

* Corresponding author: Department of Neurology, University Hospital Hradec Králové, Sokolská 581, CZ-500 05 Hradec Králové, Czech Republic; e-mail: libor.simunek@email.cz

INTRODUCTION

The association between marijuana use and the occurrence of ischemic stroke (IS) is widely discussed in the literature. Westover et al. (1) were the first who, in their extensive epidemiological study of patients admitted to Texas hospitals from 2000 to 2003, marked marijuana abuse as a risk factor for the development of IS. In 2016, Rumalla et al. (2) published a retrospective cohort study in which they analyzed data from a database of hospitalized patients in the USA between 2004 and 2011 and proved the increased likelihood of hospitalization for IS in marijuana smokers by approximately 17%. Hemachandra et al. (3) confirmed in their smaller study an increased risk of IS in marijuana smokers who use it at a frequency of at least once a week while the risk has not been proved in a smaller frequency of abuse.

In our comprehensive stroke center, 26 patients aged 15–44 (so-called "young strokes") were admitted due to IS from January 2016 to June 2017. Three of these patients reported cannabis use at least once a week in their toxicological history.

CASE REPORT 1

28-year-old male reported marijuana usage for 10 years, recently at a dose of 2–3 g of dry matter daily. He was also a tobacco cigarettes smoker (0–20 cigarettes daily). His medical history was insignificant; he did not use any medication. Stroke developed during evening rest during which the patient smoked one joint and experienced palpitation. He developed left side homonymous hemianopsia, mild central left side hemiparesis and left side hemihypoesthesia. There were no focal changes detected on brain computed tomography (CT) performed 90 min after the onset of symptoms. CT angiography (CTA) proved isolated occlusion of right posterior cerebral artery (PCA). He developed a brain infarction in the right occipital lobe with the impact of thalamus (75 × 40 × 35 mm) despite the use of the acute recanalization therapy comprising intravenous thrombolysis with the administration of 65 mg of recombinant tissue plasminogen activator (rtPA; Actilyse®, Boehringer Ingelheim, Ingelheim am Rhein, Germany) performed 145 min after symptoms onset and subsequent mechanical thrombectomy using stent-retriever (Trevo®ProVue™, Stryker, Fremont, CA, USA) performed 220 min after symptoms onset, during which the thrombembolus was partially removed and P1 and partially P2 segments were recanalized (Fig. 1), and final intra-arterial thrombolysis with the administration of 7 mg of rtPA. Left side homonymous hemianopsia and dysesthesias of the left side extremities and of the left half of the face persisted in neurological findings. The etiology of stroke was not clarified. No arrhythmia was registered both during hospitalization (bed-side monitoring of electrocardiogram [ECG]), nor during a 3-week outpatient Holter-ECG monitoring. There was no proof of cardioembolic source nor right-to-left heart shunt by transesophageal echocardiography (TEE) and a laboratory screening for thrombophilia was negative. Acetylsalicylic acid (Godasal, PRO.MED.CS, Prague,

Czech Republic) 100 mg/d was used for a secondary prevention. The patient did not experience any recurrence of neurological problems within a 1.5-year follow-up, while the previous neurological deficit persists.
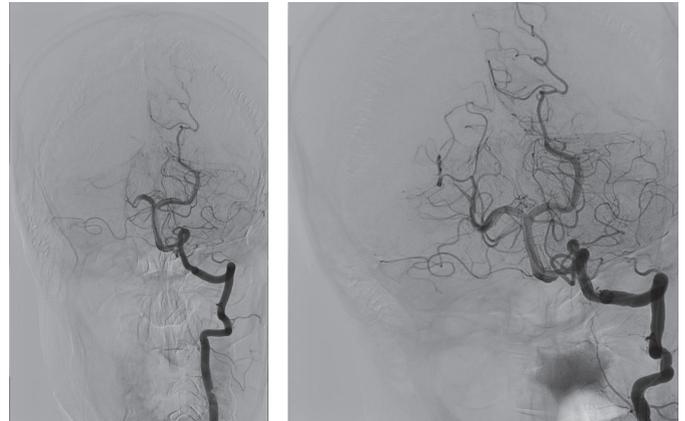

Fig. 1 Digital subtraction angiography: A) occlusion of the right posterior cerebral artery; B) final angiogram after partial recanalization of the P2 segment.

CASE REPORT 2

20-year-old healthy male claimed 6-year abuse of marijuana, in the last 4 years in a dose of 2.5 g of dry matter daily during the admission to our stroke unit. He was also an occasional ecstasy user. He sought a medical examination for 4 days lasting bulbar syndrome, right side neocerebellar syndrome and hypoesthesia of right side limbs. Magnetic resonance imaging (MRI) of the brain detected an acute infarction of the left portion of pons and mesencephalon with a diameter of 10 mm (Fig. 2). Magnetic resonance angiography (MRA) demonstrated occlusion of the central segment of basilar artery, without detection of other pathological changes. Control CTA performed after 6 days showed a stationary finding. During the examination of stroke etiology, there was persistent foramen ovale (PFO) detected on TEE and we noticed recurrent night asymptomatic bradycardia with junction rhythm at heart rate of 35 beats per minute on ECG. Ultrasound ruled out the deep venous thrombosis of the lower limbs. We suspected, that the mechanism of the IS was cardioembolic or paradoxical embolization, and therefore, anticoagulation therapy with warfarin (Orion Corporation Orionintie, Espoo, Finland) 3 mg/d was started and closure of PFO is planned. Eighteen months later, the patient is without a functionally significant deficit, still in the waiting list for the PFO closure.

CASE REPORT 3

28-year-old healthy female reported using marijuana for the last five years at a dose of 1 g of dry matter weekly at the time of admission. Several months ago she stopped smoking tobacco cigarettes. She was without medication at the time of stroke onset, half a year before she ceased using hormonal contraception after 10 years. Firstly, she was admitted to a local department of neurology due to the mild expres-

Fig. 2 Magnetic resonance imaging – fluid attenuated inversion recovery, sagittal plane: acute infarction in the pons.
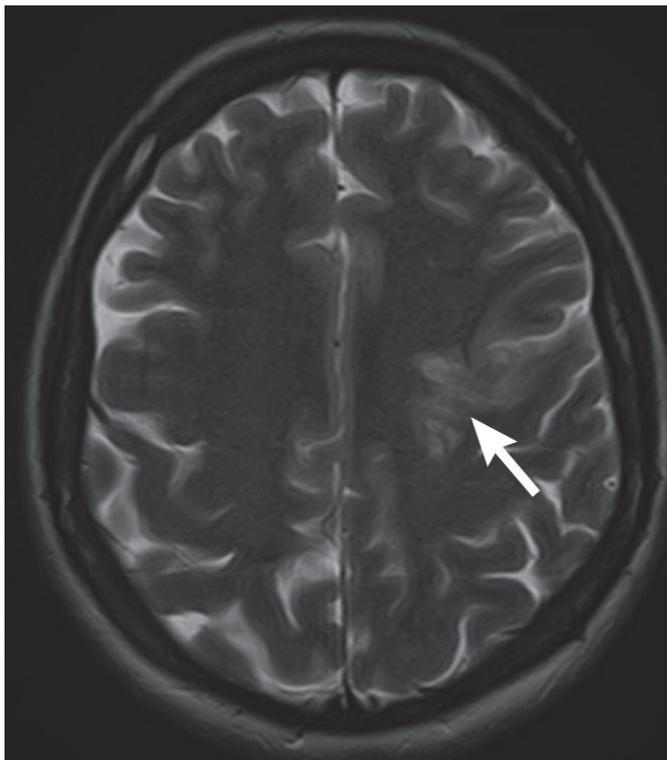

Fig. 3 Magnetic resonance imaging – T2-weighted images, transverse plane: acute infarction in the territory of the left middle cerebral artery.
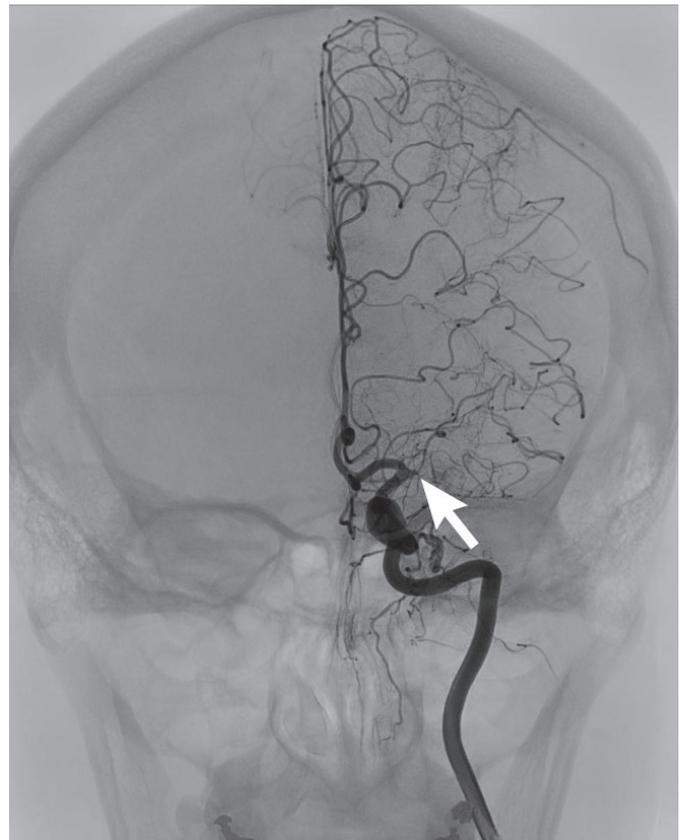

Fig. 4 Digital subtraction angiography: occlusion of the left middle cerebral artery.

cerebral artery (MCA) (Fig. 3) due to the occlusion of its M1 segment detected by MRA.

The patient was later transferred to a comprehensive stroke center, where digital subtraction angiography (DSA) confirmed the occlusion of M1 segment of the left MCA (Fig. 4) and also detected 60–70% stenosis of the intracranial segment of the left internal carotid artery. There was a collateral flow present from the left anterior cerebral artery and left PCA to the unaffected part of the left MCA territory. Well-developed collateral circulation and progression of the neurological deficit suggested a thrombogenic mechanism to the embolic one. One month lasting Holter ECG monitoring and TEE did not prove the source of cardio embolism. Laboratory screening of thrombophilic conditions proved the presence of antiphospholipidic antibodies lupus anticoagulants, APTT-LA index (activated partial tromboplastine time – lupus anticoagulant sensitive reagent) was 3.65 (with a normal ratio of 0.8–1.2). Thus, we consider IS in this patient to be a manifestation of antiphospholipid syndrome. The patient was treated with clopidogrel (Trombex, Zentiva, Prague, Czech Republic) 75 mg/d. During the following year, there was no IS reoccurrence. However, worse speech fluence persisted.

DISCUSSION

Pathophysiological mechanism of marijuana, which contributes to the development of cerebral ischemia, has not been clearly proved. The following mechanisms come to

sive dysphasia and mild right side central hemiparesis with central lesion of the right facial nerve lasting for 3 days and corresponding with the finding of cerebral infarction (2 cm in diameter) in the left frontoparietal region on admission CT. The expressive dysphasia progressed during the hospitalization, brain MRI performed three days later detected multiple ischemic lesions in the territory of the left middle

consideration: 1) cardio embolization during atrial fibrillation (AF), 2) systemic arterial hypotension, 3) reversible cerebral vasoconstriction syndrome (RCVS), and 4) less frequently vasculitis.

Marijuana usage leads to adrenergic stimulation causing the shortening of action potential of myocardium and changing its electrophysiological properties. It may lead to AF (4). Besides that, several hours following the cannabinoid application the risk of myocardial infarction increases five times (5) and this possible atrial myocardial ischemia may also contribute to the development of AF (4).

Acute marijuana use leads to tachycardia which persists for 2–3 h. Repeated exposure to marijuana leads to a gradual weakening of this effect and on the contrary leads to bradycardia. Mechanism leading to bradycardia, which has been proved on animal models, is a blockade of receptors on presynaptic endings of postganglionic fibers of the sympathetic nervous system which leads to the inhibition of sympathomimetic activity and systemic hypotension (6). We suspect a typical interterritorial localization of ischemia in the case of IS caused by systemic hypotension.

RCVS is a clinical-radiological syndrome characterized by a sudden development of a strong headache and multifocal segmental vasoconstriction of cerebral arteries. Headache can occur in an isolated episode or can reoccur within a period of 1–4 weeks. Most often it can be bilateral and may be accompanied by nausea, vomiting, photophobia and confusion (7), in some cases there is also focal neurological deficit present (8). IS belongs among other RCVS complication (8). Basic pathogenetic mechanism of RCVS is most probably defect of cerebrovascular pressure control in increased sympathomimetic reactivity, oxidative stress and endothelial dysfunction (9) may represent a significant role in pathogenesis. RCVS may be idiopathic, however, in 25–60% its occurrence is secondary (9) most often due to usage of cannabinoids or of other vasoactive substances (7). A typical finding in RCVS on CTA, MRA or DSA of cerebral arteries is a multifocal segmental arterial vasoconstriction. In most RCVS cases, correction of clinical symptoms and vasospasms occurs within 3 months (7).

As a possible cause of a higher risk of IS in marijuana smokers, toxic or autoimmune vasculitis is also less often considered in the literature. Since the 1960s, lower limbs arteritis in cannabinoid users, often leading to gangrene and amputation, has been described. However, the association of cannabinoid abuse with vasculitis of the central nervous system has not yet been described.

In our presented case reports we admit causal association between marijuana abuse and IS only in the two cases. Out of four discussed pathophysiological mechanisms related to a cannabinoid abuse, we consider in case reports 1 and 2 exclusively the cardioembolic etiology. The reason for this is the finding of the occlusion of a large cerebral artery and the absence of cerebral vessels stenosis. The possibility of cardioembolic etiology in case 1 is indirectly supported by the history of palpitation. In the second case, the finding of PFO points at a possible paradoxical embolization which would not be related to the marijuana abuse. Regarding the high PFO incidence, estimated at 34% in the age category of our patient (10), and the absence of deep venous thrombosis, we consider in our second case paradoxical embolization as a probable but not a certain etiological mechanism of IS.

CONCLUSIONS

Cannabinoid use may cause IS, especially in the younger age category. Therefore, in these patients we recommend focusing on the history of cannabinoid abuse and carry out toxicological urine tests. In marijuana chronic users, tetrahydrocannabinol can be detected in the urine for a period of 24 days after the last exposure (11).

ACKNOWLEDGEMENTS

REFERENCES

1. Westover AN, McBride S, Haley RW. Stroke in young adults who abuse amphetamines or cocaine: A population-based study of hospitalized patients. Arch Gen Psychiatry 2007; 64: 495–502.
2. Rumalla K, Reddy AY, Mittal MK. Recreational marijuana use and acute ischemic stroke: A population-based analysis of hospitalized patients in the United States. J Neurol Sci 2016; 364: 191–6.
3. Hemachandra D, McKetin R, Cherbuin N, Anstey KJ. Heavy cannabis users at elevated risk of stroke: evidence from a general population survey. Aust N Z J Public Health 2016; 40: 226–30.
4. Korantzopoulos P, Liu T, Papaioannides D, Li G, Goudevenos JA. Atrial fibrillation and marijuana smoking. Int J Clin Pract 2008; 62: 308–13.
5. Mittleman MA, Lewis RA, Maclure M, Sherwood JB, Muller JE. Triggering myocardial infarction by marijuana. Circulation 2001; 103: 2805–9.
6. Thanvi BR, Treadwell SD. Cannabis and stroke: is there a link? Postgrad Med J 2009; 85: 80–3.
7. Ducros A. Reversible cerebral vasoconstriction syndrome. Lancet Neurol 2012; 11: 906–17.
8. Šimůnek L, Smetanová L, Herzig R, Vališ M. Reversible cerebral vasoconstriction syndrome. Cesk Slov Neurol N 2017; 80(6): 708–10.
9. Miller TR, Shivashankar R, Mossa-Basha M, Gandhi D. Reversible cerebral vasoconstriction syndrome, part 1: Epidemiology, pathogenesis, and clinical course. AJNR Am J Neuroradiol 2015; 36: 1392–9.
10. Hagen PT, Scholz DG, Edwards WD. Incidence and size of patent foramen ovale during the first 10 decades of life: an autopsy study of 965 normal hearts. Mayo Clin Proc 1984; 59: 17–20.
11. Lowe RH, Abraham TT, Darwin WD, Herning R, Cadet JL, Huestis MA. Extended urinary delta9-tetrahydrocannabinol excretion in chronic cannabis users precludes use as a biomarker of new drug exposure. Drug Alcohol Depend 2009; 105: 24–32.